8

3-D forming of continuous fibre reinforcements for composites

O.K. BERGSMA, F. VAN KEULEN, A. BEUKERS, H. DE BOER AND A.A. POLYNKINE

8.1 Introduction

8.1.1 The earliest fibres, fabrics and composite structures

The control of fire and the spinning of continuous strands of fibres are probably the most important discoveries humans ever made. Both inventions made it possible for a naked human to survive in non-tropical conditions. Yarns and derivatives, like robes and textile fabrics, provided humans with a portable and personal tropical microclimate by clothes and structures so that they could withstand most climatological conditions. It made humans able to migrate from the crowded and unhealthy tropical zones to the large, cool plains and mountainous areas, free of diseases, but rich in animals, vegetables, minerals and water. Compared with animal skin, flexible textile was a big step forward. The usage of light fabrics that were adjustable to local conditions made a big and relatively fast migration of hunters and gatherers possible over all continents, except Antarctica [1]. Humans could only use local natural growing fibres. They differ from modern artificial synthetic fibres in length. Instead of the continuous filaments, nature offers only short fibres, like animal hair. These protein-based fibres are provided by animals, such as sheep, goats, camels, llamas and rabbits. Various forms of vegetable cellulose-based fibres were available as well: in a hairy form taken from seeds (cotton) and fruits (coir) or as fibres extracted from basts and leaves, like jute, sisal, hemp, flax, yucca, palm, rice, grass, ramie and rattan.

Several of these materials could instantly be used to make basket-like structures or to wattle hedges and walls. However, to handle and to make the staple fibres suitable for knitting and weaving, as shown in Fig. 8.1, the spinning and intertwining of yarns was essential. A distaff, a small portable wooden spinning wheel on a vertical axle (Fig. 8.2), had already been known in prehistoric times, far before the wooden wheel on the horizontal axle was invented to make wheeled transport possible. Depending on the local climate, people started to use ropes, felt (paper-like textile) and woven

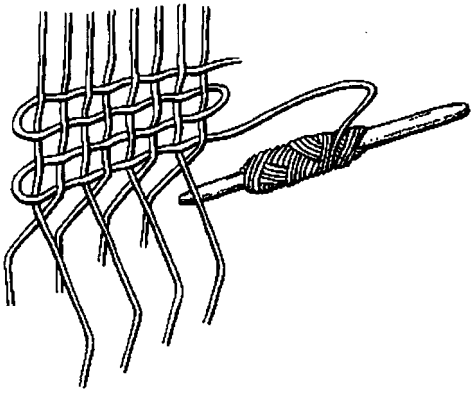

8.1 Weaving of plain fabrics.

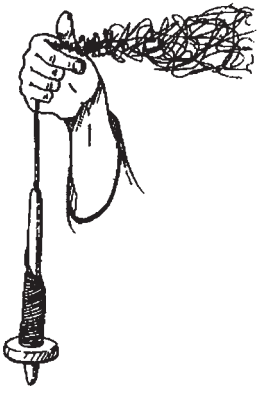

8.2 Spinning of yarns.

fabrics of different natural materials for several purposes. In many parts of the world the same ancient design of clothes, tapes, baskets and tents, all continuous fibre structures, are still in use and almost unchanged. Up to this day, 3-D textile structures still offer nomadic families the best protection against extreme temperatures. The peaked black tent, an example of a controlled draped fabric, is used in the hot dry deserts. In the cold snowy areas circular tents, yurts, are used. These circular trellis structures, limited in shear by a doorframe and a circumferential rope, are covered with wattle and felt. As soon as communities started to settle, the flexible and foldable textile structures were transformed, step by step, in more protective rigid wattle and daub or straw reinforced clay structures. In fact, it was the first creation of artificial composites, a combination of different materials to

Table 8.1. Elastic properties of some natural composites compared with steel

Material	Density ($kg/m^3 \times 10^3$)	Young's modulus ($N/m^2 \times 10^9$)	Yield stress ($N/m^2 \times 10^6$)	Yield strain (%)	Elastic energy/ weight (J/kg)
Steel					
0.2 carbon quenched	7.8	210	773	0.2	99
Piano wires, springs	7.8	210	3100	0.8	1590
Animal					
Sinew	1.3	1.24	103	4.1	1620
Buffalo horn	1.3	2.65	–124	–3.2	1530
Bovine bone	2.1	22.6	–254	–1.4	846
Ivory	1.9	17.5	217	1.2	685
Hardwood					
Ash	0.69	13.4	165	1.0	1196
Birch	0.65	16.5	137	1.0	1050
Elm	0.46	7.0	68	1.0	740
Wych elm	0.55	10.9	105	1.0	950
Oak	0.69	13.0	97	1.0	703
Softwood					
Scots pine	0.46	9.9	89	0.9	870
Taxus brevifolia	0.63	10.0	116	1.3	1100

Notes:
1 Northern hardwoods, sinew and horn were the basic structural materials for the laminated composite bows and chariots from Mesopotamia and Egypt.
2 *Taxus baccata* was used for medieval longbows.
3 Horn, a natural thermoplastic polymer was especially applied in the compression loaded areas.
4 Sinew, superior in tension, was employed for strings and bow-reinforcement; more in general it was used as a shrinking (smart) robe to encapsulate and to connect different components.

obtain improved or modified properties. The earliest laminated composite structures, like composite bows and chariots, were glued layered structures of natural composites such as wood, bone, sinew and horn [2]. They were all fibrous materials, based on cellulose, collagen and keratin, which had very specific capabilities, already discovered and understood by the prehistoric craftsman (Table 8.1).

All applications mentioned in this part of the Introduction, from textile structures more than 50 to 8 millennia ago to the composite shelters, bows and chariots from 12 to 5 millennia ago were not developed overnight, the structures were sometimes very complex and took probably centuries

of experimentation and evolution. The results are still striking for the craftsmanship, knowledge of materials and the sophisticated manufacturing processes [2]. For a successful introduction of modern artificial composites, equal understanding must be developed and supported by modern mathematical modelling and computers. Besides the application of new synthetic materials, the biggest break with the past will be the introduction of low-cost and fast manufacturing and simulation equipment to replace the time-consuming, high-priced and mystic skills of craftsmen.

8.1.2 The renaissance of fibre reinforced composites

During the second half of this century, the last decade in particular, a true revival started of using light-weight composite structures for many technical applications. In the beginning, the introduction of fibre reinforced polymers was only driven by particular electromagnetic characteristics. More than a century ago, cotton reinforced rubbers and phenolics were used for insulators. Later, glass fibre reinforced polyesters were applied for radomes, minehunters and minesweepers. In the 1980s, high-technology composites based on carbon- and aramid-fibre reinforced epoxies became popular to improve the structure performance of spacecraft, military aircraft, helicopters and all kinds of sports and racing equipment. Initially, the sky was the limit as far as the price was concerned. Nowadays, cost reduction during manufacturing and operation is the technology driver, and examples are large structures in civil applications (carbon fibre reinforcement of bridges and buildings) or in corrosive chemical or marine environments (glass fibre reinforced bridges, piers, pipes, tanks, etc.). One of the latest developments is the application of continuous fibre reinforced polymers to protect people against impact and fire and a more general tendency to design means of transport which are less damaging to our environment. Some typical examples are shown in Fig. 8.3.

Like in prehistoric times, the reinforcing fibrous materials are applied in different forms; short or continuous, as tapes, mats or plain weaves. Although the vegetable fibres mentioned earlier are gaining renewed interest, most structural applications are now reinforced with synthetic fibres with constant quality. Inorganic fibres are applied such as glass, metal and silica, organic fibres based on natural cellulose and protein polymers or synthetic fibres based on condensation or addition polymers. There are innumerable types of synthetic fibres, such as single filaments or tows, neat or post-treated, stretched or carbonized. Nowadays, the most popular reinforcing fibres with respect to price–performance are the low-cost (E) glass fibres and the high modulus (HM) aramid- and high-tenacity (HT) carbon fibres (Table 8.2).

8.3 Some typical examples of continuous fibre reinforced products.

8.1.3 Industrial manufacturing of composite components

A successful introduction of reinforced polymer materials and components depends on the availability of fast and reliable manufacturing techniques. In general, new materials are more expensive than the materials they have to compete with. Added value in mechanical, chemical or physical characteristics is only convincing when the price performance is competitive. No parameter is so determinant for the price–performance ratio of advanced structures as the cost to manufacture. Once the materials have been accepted and established, the performance per unit weight gains impor-

Table 8.2. Fibre properties of some typical natural and synthetic fibres

	Density ($kg/m^3 \times 10^3$)	Young's modulus ($N/m^2 \times 10^9$)	Tensile failure ($N/m^2 \times 10^6$)	Strain failure (%)
Natural organic polymer base				
Jute	1.46	10–25	400–800	1–2
Hemp	1.48	26–30	550–900	1–6
Flax	1.54	40–85	800–2000	3–2.4
Sisal	1.33	46	700	2–3
Coir	1.25	6	221	15–40
Cotton	1.51	1–12	400–900	3–10
Synthetic organic polymer base				
HT carbon (T300)	1.76	230	3530	1.5
HM carbon (M40)	1.83	392	2740	0.7
HM aramide	1.45	133	3500	2.7
Inorganic base				
E-glass	2.58	73	3450	4.8
S/R-glass	2.48	88	4590	5.4

Note: Properties of natural materials are very variable, so the figures shown are averages and collected from a great variety of publications.

tance. Decreasing structural weight, often beneficial for performance improvement, not only reduces the quantity and cost of materials but also often reduces the production time, and consequently the cost of manufacturing. A powerful approach to reach this goal is the matrix reinforcement with proper fibres, to high possible volume fractions, continuous and with a complete control of fibre orientations, in other words to control anisotropy. The success of composite applications, by volume and by number, can be ranked by the success of the applied manufacturing techniques (Fig. 8.4). For all processes shown, suitable for short to continuous fibres, the introductory (pioneering) period was based on thermosetting polymers, from phenolics, polyesters, vinylesters to epoxies. In the case of injection moulding with short (<10 mm) and pressing with longer fibre reinforcements (<100 mm), thermoset polymers are being increasingly replaced by more expensive but technically equivalent or better thermoplastics. However, the main reason for this is the cost reduction by cycle time reduction. Most important among the technologies mentioned is injection moulding of generally small and complex parts. The reinforcement by fibres is limited with respect to length, volume percentage (<35%) and orientation control. Flow-moulding of larger thermoset and thermoplastic shell-structures (SMC and GMT) became important as well, especially for car

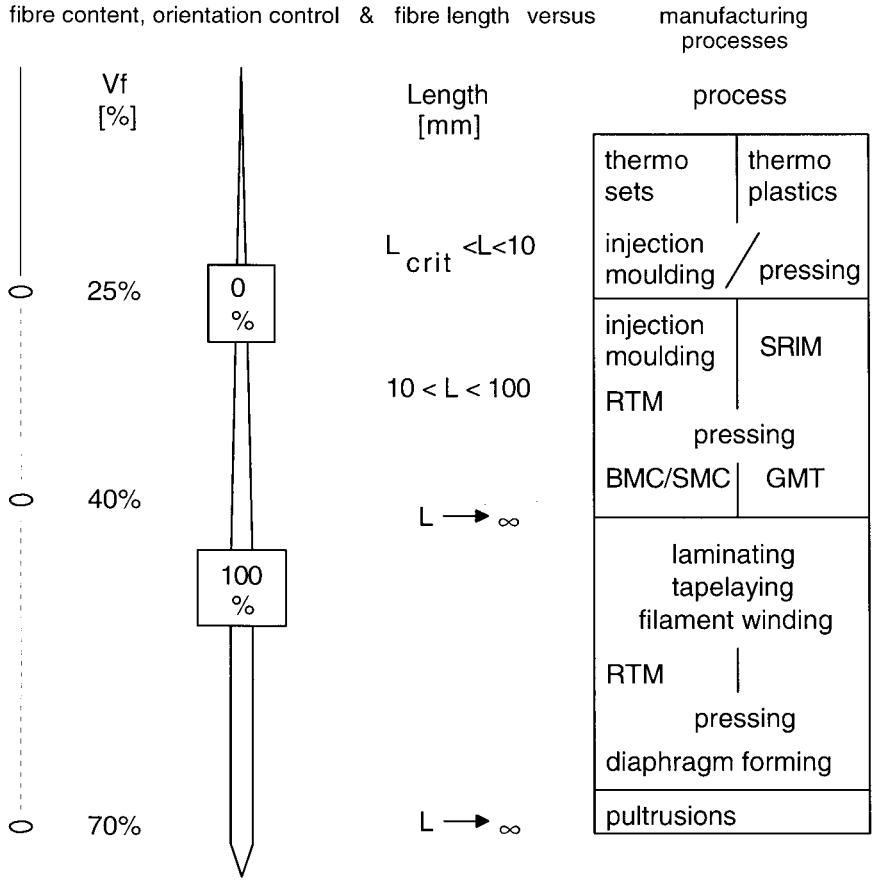

8.4 Industrial manufacturing techniques.

parts. The length (<100 mm) and volume percentage (<45%) of the reinforcing fibres increase. The control of fibre orientations is similar to injection moulding, limited to keeping fibres as random and uniformly distributed as possible. In the case of modern advanced structures (high loads, low weight), where controlled fibre placement is essential, designers and manufacturers still rely on techniques that are labour or capital intensive (laminating by hand or the use of dedicated equipment). In the case of some advanced composite applications, human labour is only replaced by cost reducing and accurate machines in the stage of pre-impregnation and the cutting of patches. Industrial laminating by tape or fabric laying machines is still limited to a few (aircraft) shell structures. The most successful techniques in terms of volume usage are the filament winding of

pressure vessels and the pultrusion of composite profiles. Typical for the advanced composite sector is the use of continuous fibres (glass, aramid and carbon) and the high fibre volume percentages (<70%). It is still the domain of thermosetting polymers.

Although the application of advanced continuous fibre reinforced composites may result in highly satisfactory structural performances [3], the volume and number of applications are still limited. The success of the advanced composites depends completely on the availability of fast and reproducible industrial manufacturing processes.

A development of such an industrial process based on 3-D deformation, i.e. draping, of (impregnated) textile fabrics, is the subject of this chapter. The major deformation mechanisms, the geometrical draping–simulation strategies, finite element simulation and the final product optimization, essential for designers and analysts, is outlined in the following sections.

The draping process is part of a press-forming cycle, more specifically the press forming of textile fabrics which are impregnated to a certain extent with thermosetting or preferably thermoplastic polymers. Nowadays many industrial impregnation strategies for both thermosetting or thermoplastic polymers are available. Once the fabric has been impregnated and the polymer brought to a deformable state, e.g. by heating, the plain sheet can be formed into a shell structure in seconds by press forming and (re)consolidation in the last phase by application of matching dies. This technology can be used to produce high-quality preforms for the (thermosetting) resin injection or transfer moulding (RTM) of advanced aircraft and car components (Fig. 8.4). Major successes are, however, achieved in the press forming of continuous reinforced thermoplastic composite parts (Figs. 8.5 and 8.6). Similar to the already-mentioned technologies for advanced composites, high fibre volume contents and reproducible fibre orientations are typical for press forming. The speed is comparable with the ordinary injection moulding and flow-moulding of short fibre reinforced parts. The pressure levels are relatively low: for forming, 1 bar or less; for (re-) consolidation, 10–40 bar. When the heating and cooling times are considered as well (for thin-walled structures, a matter of seconds), it is clear that the press forming of advanced composites is not only attractive because of its manufacturing speed, but also because of the light-weight equipment and minimum energy required [4].

8.1.4 Outline of the simulation and optimization strategy

The following sections deal with the simulation and optimization of 3-D formed continuous fibre reinforced components. In the scheme shown in Fig. 8.5 the role they play in an integral process of design and analysis is clarified. When automated structural optimization is applied, the scheme

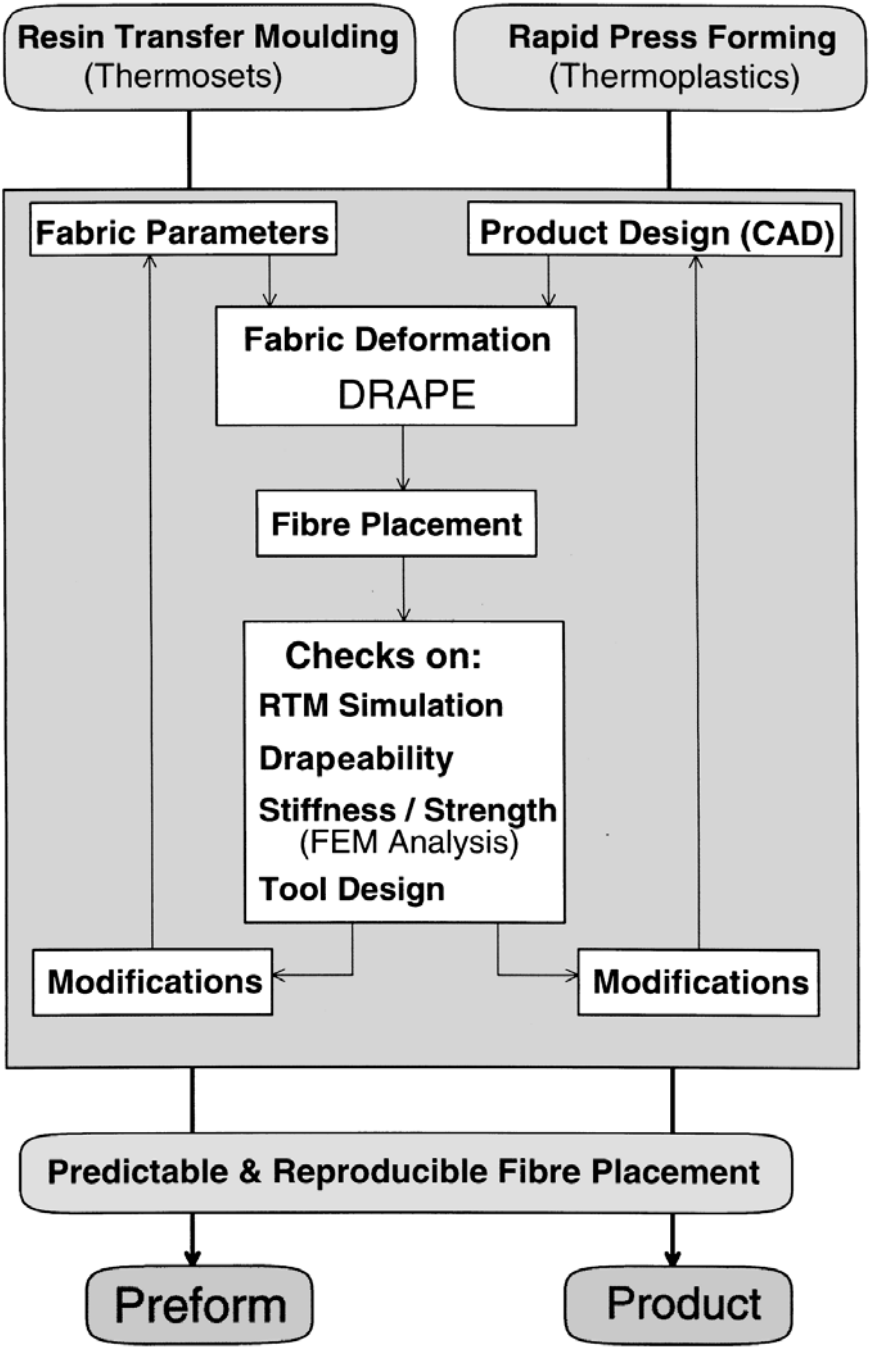

8.5 Design of advanced composite shell structures.

a)

b)

8.6 Typical continuous fibre reinforced products, manufactured using a thermoforming process: (a) automotive chassis part; (b) bicycle wheel.

will alter somewhat, as the entire process must be controlled by the applied optimizer (see Fig. 8.19).

A general description of thermoforming of continuous fibre reinforced thermoplastic (CFRTP) products is given in Section 8.2. Numerical simulation of the forming process is the topic of Section 8.3. In this section, the discussion is mainly restricted to geometrical approaches. This choice has

been made because this type of simulation requires modest computer effort and is therefore especially suited for optimization processes. In addition to the simulation of the forming processes, the evaluation of design sensitivities is considered as well. Simulation of the mechanical behaviour of CFRTP products is discussed in Section 8.4, although the discussion is restricted to thin-walled structures. As descriptions of the finite element method can be found in many textbooks, this discussion is restricted. However, the evaluation of the required laminate stiffnesses is non-standard and is therefore included in the present chapter. Automated optimization is addressed in Section 8.5. Here, optimization is carried out on the basis of a so-called approximation concept. This approach replaces the actual optimization problem by a sequence of simpler approximate optimization problems. The main advantages of this approximation concept are: (1) it is applicable without information on design sensitivities and (2) noisy response evaluations can be dealt with.

8.2 Forming of continuous fibre reinforced polymers

8.2.1 Introduction

With the development of high-performance continuous fibre reinforced polymers, the need for new production processes became clear. Hand lay-up, the most important production process for continuous fibre reinforced thermoset structures, is not suitable for most thermoplastic composites. This and the fact that large numbers produced with the hand lay-up process cannot lead to cost-competitive products, are the main reasons for the development of new industrial production techniques for composite materials. Some pressing processes have the potential of becoming cheap and fast, and are therefore suitable for mass production.

In this section only the rubber forming process will be discussed, since this low-pressure form pressing process seems among the most promising of its kind.

8.2.2 Rubber forming

The rubber forming process is a matched die press forming process. One of the dies, male or female, consists of rubber. Figure 8.7 gives a general outline of the rubber forming process. The important stages in the forming process are:

- preconsolidation (depending on the prepreg type);
- heating stage (can be included in the preconsolidation stage);
- forming stage (draping);
- (re)consolidation stage.

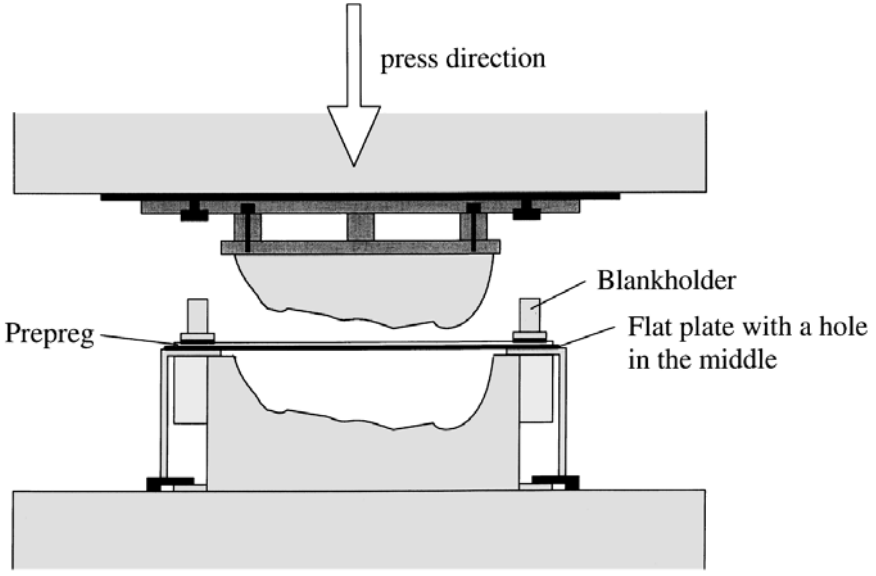

8.7 A sketch of the rubber forming process.

Heating stage

The laminate can be heated by contact heat (conduction heating) between two hot plates. When this is done with sufficient pressure, pre-consolidation can become unnecessary [5]. A disadvantage of the conduction heating method is the fact that the laminate actually touches the heating equipment. Consequently, good release agents must be used to prevent sticking of the material to the plates.

Convection heating in an oven is also possible, but will usually be time consuming, and the use of inert gas is sometimes necessary to prevent oxidation of the polymer at high temperatures. Inert gas environments are also recommended when using the very fast infrared heating methods. A disadvantage is that for thick sheets temperature gradients develop through the thickness and this will sometimes restrain formability during the forming stage. Radiation heating, however, is a clean and quick heating method in general. It provides a flexible and a well-manageable heating device.

Forming stage

When a fabric reinforced thermoplastic laminate is forced in a specific shape by the rubber forming process, the fibre reinforcement has to adjust to that same shape. The continuity of the fibres plays an essential role. In

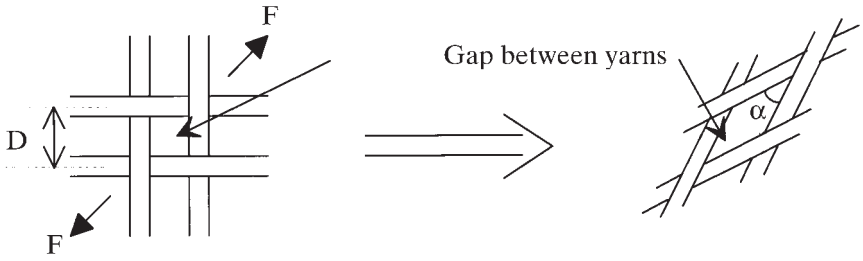

8.8 Schematic drawing of the intraply shear deformation mode.

contrast to metals or nonreinforced thermoplastics, continuous fibre reinforced plastics cannot undergo a deformation with only local adjustment of the material. Local bending or curving of the laminate material will influence the entire laminate. There are several ways in which the adjustments of the fibre reinforcement can take place. These adjustments are often called deformation modes.

Although composite products generally are composed of laminates, that is to say of more than one layer, the deformation capacity of one individual layer plays a dominant role in the forming process. These deformations are called *intraply* deformations. In general, five different deformation modes of a single, flat layer of fabric can be identified, as was shown by Mack and Taylor [6], Robertson *et al*. [7], Heisey and Haller [8] and Robroek [4]:

- fibre stretching (elongation of the fibres);
- fibre straightening (undulation of the woven fibres);
- intraply shearing (trellis effect of the fibres);
- intraply slip (sliding of the fibres);
- bucking (in-plane and out-of-plane buckling).

As has already been shown by Robertson *et al.* [7] and confirmed by Potter [9] and Van West [10], the shear deformation mode (Fig. 8.8) is the most important mode for deforming fabrics into 3-D products. Simulations as discussed in the next section must therefore incorporate this deformation mode.

Since the shearing dominates the deformation, it is important to know which forces are needed for the shearing. It appears [4] that the forming forces of these fabric reinforced plastics are small. Normally, a laminate consists of more than one layer. Such a laminate can be represented as a stack of fibre-rich layers alternated with thermoplastic resin-rich layers. In a thermoforming process (such as rubber forming), the resin-rich layers are softened by heating and will have a certain viscosity. They will allow the fibre-rich layers to slip with respect to each other when the laminate is bent

8.9 Schematic drawing of the interply shear deformation mode.

by forming forces. This deformation mode is called *interply* slipping (Fig. 8.9). During this slipping the resin-rich layer must act as a lubricant, otherwise the generated tangential stresses become too high and can cause failure of the laminate bend [11].

Since the pressures needed for the forming are relatively low (<1 bar during forming, <40 bar in the final consolidation stage), tooling materials other than the ones used in a metal, matched die, forming process become feasible. The thickness of the fabric after deforming is mainly determined by the local amount of shear [5]. When this thickness variation is obstructed, high pressures on the fabric will occur, which will obstruct the shearing of the fabric. Therefore, the gap between the male and female dies should not be constant in general, and a variation in the thickness must be allowed. A relatively simple way to accomplish this is to use a die made from a relatively soft material. This material should deform at places where the thickness varies. Another way of avoiding high local pressures is by adapting the shape of one of the moulds to the thickness variation. Since the increase in thickness is directly related to the deformation of the laminate, a detailed simulation of the fabric deformation is in that case essential for the design of the dies.

Suitable materials for the relatively soft moulds are silicon rubbers, since they can withstand high temperatures for short periods (temperatures higher than 400 °C). The hardness of the silicon rubber is variable between 55 Shore A and 73 Shore A. A disadvantage of silicon rubber is that it is notch-sensitive. For lower temperature rubber forming processes (temperature lower than 250 °C) it is therefore preferable to use a tougher material, for instance PU (polyurethane) rubber [5].

The choice for a rubber male of female die depends on the product. The quality of the surface that is in contact with the metal die ranges from textured to super glossy. The surface that touches the rubber die is rough, in general. In most cases this determines which die should be made of rubber. At present most products are made with a metal female and a rubber male die.

A disadvantage, related to the use of rubber as male die material, is that the shape of the die itself can change before the consolidation stage of the thermoplastic composite. This easily leads to folds and wrinkles. It can also lead to the unwanted effect of fibre bridging, as shown in Fig. 8.10. At places

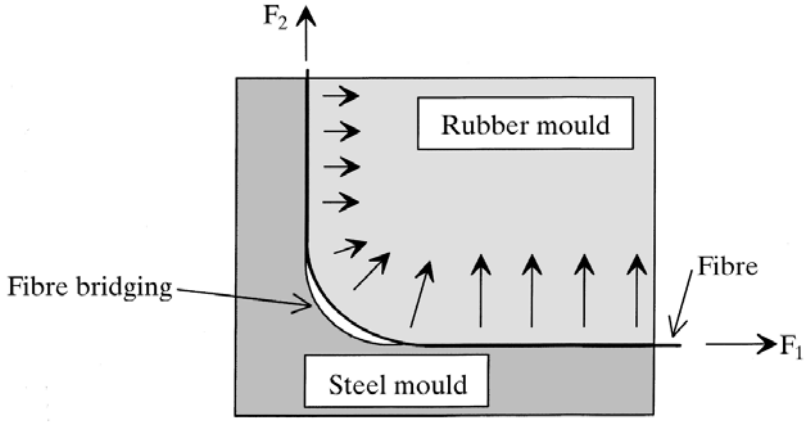

8.10 The yarns of the fabric deform the rubber mould.

where a large curvature of the surface is found, the fibres of the fabric will try to bridge the corner, resulting in an undefined shape of the product. To overcome this problem, extra rubber can be added locally.

If preference is given to a metal male die and a rubber female die, the shape of the product cannot become undefined. Obtaining the proper pressure distribution for consolidation is often the main problem in this case. For mass production the only matching die candidate materials are metals.

The function of the clamping device, also referred to as the buckling guide or blankholder, is different from similar metal forming processes. Although it is meant to prevent out-of-plane deformations of the laminate, the primary function of the guide is to make sure that the fibres are under tension during the forming process in order to avoid in-plane, rather than out-of-plane, buckling. Hence the buckling guide should act as a steering device.

The forming of the product is governed by the pressure distribution on the laminate. Large local deformations, for instance near corners, can be stimulated by increasing the pressure locally. By using a clamping device the friction forces can be controlled. If the friction forces are not capable of deforming the fabric sufficiently, pins, locking the fabric at certain places, can also be used. Unfortunately, the forces exerted by these pins also result in a tearing of the fabric in the vicinity of the pins. It is therefore inevitable that the pins are placed at positions that remain outside the product, resulting in extra scrap material.

Usually the fabric is placed on a supporting plate (Fig. 8.7). The fabric is held at the edges by the blankholder, i.e. the fabric is not supported in the middle. When the fabric is heated by conduction, the hole in the support-

ing plate should be filled with a matching plate. This is to ensure a homogeneous temperature.

(P)reconsolidation stage

After the heating stage of the blank and the stage of product forming via intraply shear, bending and interply slip, the deformed shell laminae must be reconsolidated in a final solidification stage. The state of impregnation and adhesion is determinant for the final cycle of closed mould pressure and temperature. In the case of poorly impregnated fibres and fabrics, like the commingled, co-woven or powder impregnated polymer–fibre combinations, a preconsolidation of the laminate blanks can be inevitable. The fibres are properly impregnated with a viscous polymer and several layers of prepreg are bonded together by heat and pressure over a period of time, batchwise in a hot platen press or continuous in a double belt press. In that case of preimpregnation techniques based on solvent impregnation or (powder- or film-)melt impregnation a preconsolidation is no longer necessary. In that case, the heating, forming and final consolidation cycle of rubber forming takes less than a few minutes per part. In the case of mass production, where the forming cycle must be as short as possible, it is favourable to carry out a part of the impregnation and consolidation outside the real rubber forming cycle. Several prepreg materials are supplied in a state of partial or total consolidation [12]. The cost saving by deleting the preconsolidation stage and the reduction of cycle time is in general balanced by a higher material price. A disadvantage of preconsolidated sheets is that they have to be supplied in the right configuration (lay-up and thickness) for each specific product.

8.3 Simulation of the forming process

8.3.1 Introduction

Simulations of forming processes are required for several reasons. Firstly, questions regarding manufacturability should be answered in a cost-effective manner. Often, the way of checking the manufacturability is by testing. In general, tests require long processing times, since tooling prototypes have to be manufactured and modified. Moreover, as testing is labour intensive, large costs may be involved. In such a setting, adaptations of the design are typically developed by trial-and-error. When these trial-and-error processes can be replaced by automated optimization processes, both the time to market and the amount of money spent in the design process can be reduced significantly.

A second requirement for forming simulation techniques emerges from

the point of view of structural analysis. If structural analysis is to be performed for continuous fibre reinforced products, information on local material properties is a necessity. A typical example is the local fibre orientations. The latter are required when laminate stiffnesses have to be calculated.

Geometric predictions were carried out as early as 1956, when Mack and Taylor [6] showed how a continuous, differentiable surface of revolution can be covered with fabric. They concluded that the shear deformation mode is the most important in-plane deformation mode during the draping of fabrics. They also concluded that, as far as the shear deformation mode is concerned, the fabric behaviour is similar to the behaviour of a fisherman's net, with the crossover points of warp and weft fibres as pivoting points.

In general, geometric approaches assume that the thermoforming process is dominated by certain deformation modes of the reinforcing fabric. For this purpose the only deformation modes taken into account are intraply shear and bending. In the case of multiple layers, interply shear is allowed as well. Other deformation modes, such as fibre stretching, wrinkling and slip at crossover points, are not taken into account. These assumptions are quite commonly accepted [6–8,10,13]. It was shown that, generally speaking, a geometric simulation based on these assumptions can predict the local fibre orientations sufficiently accurately. By neglecting certain deformation modes, such as fibre stretching and wrinkling, the problem of finding the fibre orientations in the thermoformed configuration simplifies significantly. Clearly, each neglected deformation mode introduces additional constraints, which consequently reduce the number of unknowns of the forming problem at hand.

Pioneering work on geometric approaches towards the simulation of thermoforming has been done by Bergsma and Huisman [14] and Van West *et al.* [15], among others. Both approaches start out with the definition of an initial warp and weft yarn. Subsequently, the remaining crossover points are found using the yarn's inextensibility. A similar approach, but formulated in a more mathematical framework, is presented by Gutowski *et al.* [16]. The work of Van der Weeën [17] can be classified in the same group. The basic assumption is again that the only significant deformations are intraply shear and bending. In [17], the inextensibility constraints are, however, handled in three distinct ways. The first method is based on an energy approach. In this formulation the distance between crossover points is kept constant by trying to minimize the elastic energy in a single cell. This elastic energy is determined by the deformations in the yarn directions. The second approach tries to simulate the behaviour of an angler's net. A cell is completed with line segments which run along geodetic lines. The integration along these geodetic lines makes the method expensive. Whereas

the first two methods operate on curved surfaces, the third method described in [17] is intended for kinked surfaces. In the work of Trochu *et al*. [18] special attention is paid to an efficient method for describing the geometry at hand. The simulation of the draping process is basically the same as for other geometrically oriented methods. Noteworthy is the work by Aono *et al*. [19]. In [19] the effect of triangular darts has been incorporated as well. Later, the formulation was refined to distinguish between stitched and trimmed darts [20].

Most of the above geometrical approaches apply a choice for the locations of the first warp and weft yarn. Bergsma [21] attempted to avoid this initial guess. Bergsma's algorithm applies a so-called 'strategy'. This strategy provides a scheme that is used to add cells of the fabric during the simulation of the forming process. In [21] several strategies are reported and tested. In the context of design optimization, these strategies have the disadvantage that the evaluation of design sensitivities becomes somewhat more difficult.

The major advantage of the geometric approaches is the fact that with little computational effort a good indication of the fibre orientations and manufacturability can be obtained. However, important effects, such as temperature effects, friction, interply shear, wrinkling and all effects related to the matrix material, are not incorporated.

More accurate and detailed simulation results for forming processes can be obtained by using finite element models. An early application of finite element techniques to the modelling of cloth can be found in the work of Terzopoulos and Fleischer [22]. In there, the modelling was mainly used to achieve more realistic computer graphics. Among the early research devoted to the draping behaviour of fabrics was the work of Collier *et al.* [23]. Here, non-linear shell elements were applied in combination with orthotropic material behaviour. Only a single layer fabric without matrix material was used. Finite element models attempting more realistic simulations of thermoforming processes have been described in [24–26]. In Pickett *et al.* [24], stacking of shell elements was applied in an explicit finite element model. Both intra- and interply shear effects were taken into account. A uniform temperature distribution was applied. In De Luca *et al*. [25] the model of Pickett *et al.* [24] was further refined by the introduction of heat conduction. A similar approach was described by Johnson and Pickett [26].

With the detailed finite element models reported in [25,26], realistic results can be obtained. The required computer times are still relatively high, however. Particularly in the design stage or when automated optimization strategies are applied and many intermediate designs must be evaluated, this aspect may become prohibitive. For that reason, the present discussion will be restricted to geometrically based algorithms only.

In general, structural optimization algorithms become much more efficient when design sensitivities [27] are available. Moreover, the availability of design sensitivities is also advantageous in the context of geometrical thermoforming simulations. When (design) sensitivities are available, it is possible to introduce an entirely new class of strategies. These can be based on the application of iterative processes that attempt to satisfy, iteratively, additional constraints and/or to minimize a global objective function. Such constraints can, for example, reflect a maximum shearing angle (locking angle) or constraints due to position pens. A typical objective function could be the *estimated* dissipated energy or the average shear angle. Hence, a fabric will be relocated in an iterative manner, until all constraints are satisfied and/or a characteristic function is minimized.

The outline of the present section is as follows. Firstly, the geometric approach proposed by Bergsma [21] will be summarized. As this approach has some disadvantages in the context of structural optimization, a more classical geometric approach will then be described. In addition, the evaluation of design sensitivities will be described. Finally, some numerical examples will be presented.

8.3.2 Strategy approach

Since interply interaction is neglected in a geometrical simulation, the present section will address single layer fabrics only. Multiple layers can be accounted for by stacking them on each other.

The most commonly used method is based on an initial selection of the position of initial warp and weft yarns. This is depicted in Fig. 8.11. Typical approaches are to start with two orthogonal directions in a starting point and to define the initial warp and weft yarns as geodetic lines. All remain-

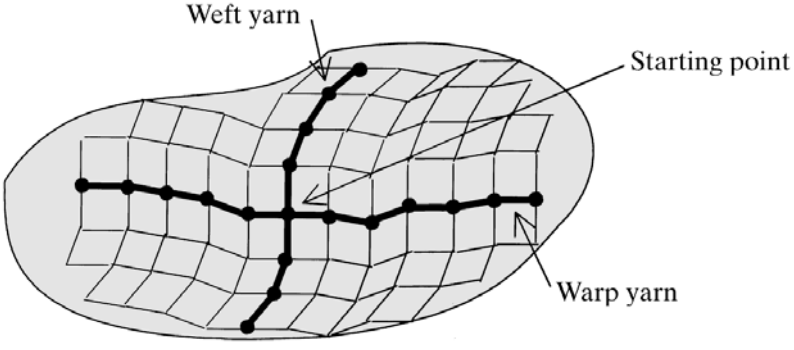

8.11 The fabric is uniquely defined when the positions of a single warp yarn and weft yarn are well known.

ing grid points are now found using the inextensibility constraint. In contrast to this approach, Bergsma [21] used a so-called *strategy* for selecting a grid point where a new set of cells (incomplete row or column) must be added. The strategy also prescribes the shear angles of the newly introduced cells. This approach is depicted in Fig. 8.12. Note that without using a strategy, there are infinite possibilities to cover the product shape with the fabric. Only a few of them are physically acceptable. The strategy introduces additional constraints reducing the degree of freedom of the fabric. Hence, the uniqueness and the quality of the obtained solution are fully determined by the applied strategy.

In order to illustrate the strategy approach, the strategy used for rubber forming of continuous fibre reinforced products will be discussed. It should be mentioned that in this case the strategy basically reflects the applied production process and is based on experimental observations. Proper formulation is therefore difficult and cannot be rigorously proven to be correct. Experimental observations show that during the rubber forming the fabric gradually contacts the mould surface. Pieces of the fabric that touch the die cannot move easily over it, since it is often cold, and the viscous matrix will cool and solidify. Moreover, the rubber die presses the fabric onto the mould surface, which leads to increased friction forces. Note that when using a heated mould, it is necessary to reformulate the strategy. Based on these observations, the present strategy is to find points that will be in contact first and will consequently define the corresponding fibre direction. This requires the following three subsequent steps:

1 Find the yarn segment of the fabric that is expected to be in contact with the product shape. This is done by comparing all possible pieces of yarn

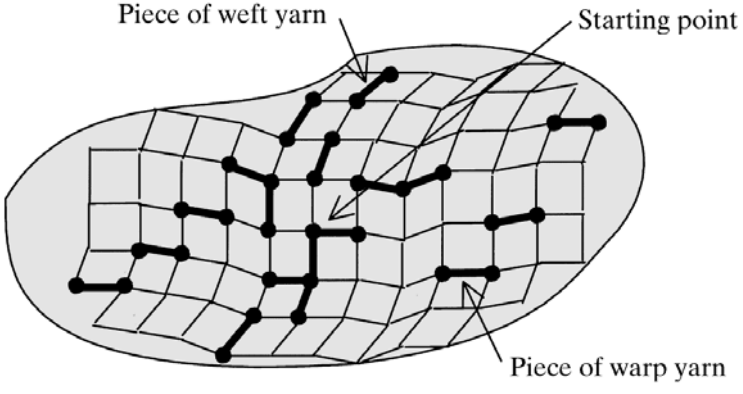

8.12 The pieces of yarn that define the unique covering do not have to be part of a single warp or weft yarn.

that are almost of the product shape and decide which one is closest to the product shape.
2 Find the expected direction of this piece of yarn. This is done by combining the direction of the part of the yarn that is already draped and the direction of the driving force of the forming.
3 Calculate the new crossover point as defined by this piece of yarn. This is done by using the inextensibility condition and the fact that the new crossover point must be located on the die.

This way of calculating a new cell of the fabric can be repeated until the whole product shape is covered with fabric.

The major advantage of this approach is that it gives a good reflection of the production process, especially in comparison with other geometrical approaches. However, the strategy approach has two disadvantages. Firstly, for every production process a strategy has to be defined, which can be very difficult for certain processes [21]. Secondly, the evaluation of design sensitivities is somewhat difficult.

8.3.3 Integration approach

In a structural optimization setting, it is more convenient to start with positioning a single warp and weft yarn. As the placement of the first two yarns is computed by numerical integration, this approach will be denoted *integration* approach. The positions of these two yarns are considered as independent quantities, although, of course, constrained by the yarn inextensibility. Furthermore, the positions are controlled by an appropriate set of (design) variables. In this paragraph no distinction will be made between the first warp and weft yarn. The presented results are applicable to both.

It is assumed that the surface consists of a collection of branches, each having its own geometric description, possibly on the basis of simple surfaces, e.g. Coons patches and cylindrical and spherical surfaces. The entire surface is finally determined by

$$S(\boldsymbol{x}, \boldsymbol{d}) = 0, \quad \boldsymbol{x} \in R^3 \qquad [8.1]$$

where $\boldsymbol{d}$ is a vector of design variables. Moreover, it is assumed that for each branch a surface description with curvilinear coordinates is available. These coordinates may be discontinuous at interfaces between adjacent branches. For convenience we assume for each $\boldsymbol{x}$, which satisfies 8.1, a set of unique surface coordinates a^α, $\alpha = 1, 2$, such that

$$\boldsymbol{x} = \boldsymbol{R}_b(a^\alpha, \mathbf{d}) \qquad [8.2]$$

where the subscript b refers to a particular branch. A normal vector to the surface will be formulated as

$$\boldsymbol{n} = \mu \frac{\partial}{\partial \boldsymbol{x}}(S), \text{ where } \mu = \left\| \frac{\partial S}{\partial \boldsymbol{x}} \right\|^{-1} \quad [8.3]$$

For each yarn a material coordinate y is introduced. The position of the yarn is assumed to be given by $\boldsymbol{R}(y, \boldsymbol{d})$. The corresponding tangent vector is defined as

$$\boldsymbol{i} = \frac{\partial \boldsymbol{R}}{\partial y} = \boldsymbol{R}_y \quad [8.4]$$

A set of local basis vectors is completed by defining a vector $\boldsymbol{j}$ as follows:

$$\boldsymbol{i} \times \boldsymbol{j} = \boldsymbol{n}, \quad \boldsymbol{i} \cdot \boldsymbol{j} = 0 \quad [8.5]$$

The material coordinate y is taken as the length measured along the yarn. Since the yarns cannot be extended, it consequently holds that $\boldsymbol{i} \cdot \boldsymbol{i} = \boldsymbol{j} \cdot \boldsymbol{j} = 1$. In order to control the position of the first yarn, it seems convenient to introduce a function $P(y, \boldsymbol{d})$, which specifies the orientation by

$$P(y, \boldsymbol{d}) = \boldsymbol{i}_y \cdot \boldsymbol{j} \quad [8.6]$$

Hence P is a measure for the curvature of the yarn in the tangent plane. Note that an initial guess for P must be given in advance. The correct value of P can be computed iteratively by imposing additional constraints or by formulating the simulation as an optimization problem as discussed in the Introduction. Thus, the applied constraint functions and/or objective function basically reflect the forming process. This means that each forming process requires the formulation of a set of constraint functions and/or objective function, without affecting the actual implementation. The function P can be controlled by an additional set of parameters.

Coming back to Equation 8.6,

$$\boldsymbol{i}_y = P\boldsymbol{j} - (\boldsymbol{i} \cdot \boldsymbol{n}_y)\boldsymbol{n} \quad [8.7]$$

Integration of 8.4 and 8.7, using the initial conditions $\boldsymbol{x}(y = 0, \boldsymbol{d}) = \boldsymbol{R}^0(\boldsymbol{d})$ and $\boldsymbol{i}(y = 0, \boldsymbol{d}) = \boldsymbol{i}^0(\boldsymbol{d})$, yields the locations and orientations of the first yarn as a function of the co-ordinate y. Here, the initial conditions specify the location and orientation at $y = 0$, respectively.

Once single warp and weft yarns have been specified, the locations of the remaining yarns can be found in a straightforward manner. At this point, it is necessary to distinguish between warp and weft yarns. All quantities related to the warp yarns will be denoted by $\overline{\ldots}$. Consider the point of intersection of two yarns which is determined by $\overline{\boldsymbol{R}}(\overline{y_1}, \boldsymbol{d}) = \boldsymbol{R}(y_1, \boldsymbol{d})$. For both yarns, increments of the co-ordinates $\overline{y}$ and y are introduced as $\overline{\Delta}$ and Δ, respectively.

After the introduction of $\overline{\Delta}$ and Δ, parts of the adjacent yarns can be constructed, as depicted in Fig. 8.13. A new crossover point is constructed,

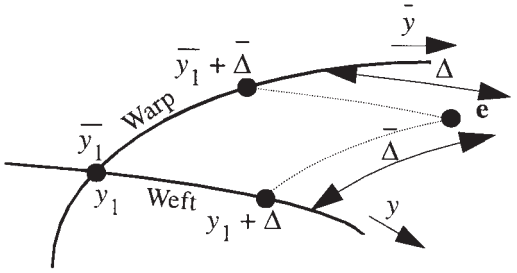

8.13 Evaluation of new crossover points and adjacent yarn segments. The new yarn segments are plotted with dotted lines.

which is denoted as $\boldsymbol{e}$, as shown in Fig. 8.13. When $\bar{\Delta}$ and Δ are sufficiently small, inextensibility of both yarns yields

$$\left[\boldsymbol{e} - \overline{\boldsymbol{R}}\left(\overline{y_1} + \bar{\Delta}, \boldsymbol{d}\right)\right] \cdot \left[\boldsymbol{e} - \overline{\boldsymbol{R}}\left(\overline{y_1} + \bar{\Delta}, \boldsymbol{d}\right)\right] = \Delta^2 \qquad [8.8]$$

$$[\boldsymbol{e} - \boldsymbol{R}(y_1 + \Delta, \boldsymbol{d})] \cdot [\boldsymbol{e} - \boldsymbol{R}(y_1 + \Delta, \boldsymbol{d})] = \bar{\Delta}^2 \qquad [8.9]$$

Moreover, the new crossover point $\boldsymbol{e}$ should be located on the die. Therefore, the condition $S(\boldsymbol{e}, \boldsymbol{d}) = 0$ has to be satisfied. The precise location of $\boldsymbol{e}$ can be determined iteratively using a Newton process. With a successive application of the above equations, the entire fabric can be constructed, as soon as initial warp and weft yarns are determined.

8.3.4 Design sensitivities

In general, the derivative of a characteristic function with respect to a design variable is called a *design sensitivity*. In a structural optimization setting, it is useful to know how the draped fabric will re-orient if the shape of the product or the initial fabric orientation changes. That is, one wants to know the design sensitivity of, for example, the local fibre orientation with respect to a characteristic product dimension.

As mentioned before, it is also useful to have sensitivities at hand within the context of thermoforming simulations. Suppose the function P, defined by 8.6, to be determined by a variable. This function has to be specified in advance, but obviously is not known *a priori*. The basic idea of the integration approach is to use an initial guess for P and to compute the corresponding fibre placement and sensitivities. Using the sensitivity information, a better guess for the function P can be formulated. This iterative process will be continued until all constraints are satisfied and/or a characteristic function is minimized.

Design sensitivities on the basis of the integration approach can be obtained rather easily. To achieve a compact notation, partial derivatives

with respect to a design variable are introduced as $\partial \ldots / \partial d_k = \ldots^*$. For the first warp and weft yarns, using 8.4, 8.7 and $\boldsymbol{j} = \boldsymbol{n} \times \boldsymbol{i}$, follows

$$\boldsymbol{i}^*_y = \boldsymbol{R}^*_{yy} = P^*\boldsymbol{j} + P(\boldsymbol{n}^* \times \boldsymbol{i} + \boldsymbol{n} \times \boldsymbol{i}^*) - (\boldsymbol{i}^* \cdot \boldsymbol{n}_y + \boldsymbol{i} \cdot \boldsymbol{n}^*_y)\boldsymbol{n} - (\boldsymbol{i} \cdot \boldsymbol{n}_y)\boldsymbol{n}^* \quad [8.10]$$

while corresponding initial conditions are formulated as $\boldsymbol{x}^*(0, \boldsymbol{d}) = \boldsymbol{R}^{0*}$ and $\boldsymbol{i}^*(0, \boldsymbol{d}) = \boldsymbol{i}^{0*}$, respectively. Note that 8.10 provides a basis for determining $\boldsymbol{R}^*$, or equivalently $\boldsymbol{x}^*$, and $\boldsymbol{i}^*$ by means of (numerical) integration.

Design sensitivities for the entire fabric can be formulated on the basis of 8.8, 8.9 and $S(\boldsymbol{e}, \boldsymbol{d}) = 0$. Straightforward differentiation yields

$$\left[\boldsymbol{e} - \overline{\boldsymbol{R}}\left(\overline{y_1} + \overline{\Delta}, \boldsymbol{d}\right)\right] \cdot \left[\boldsymbol{e}^* - \overline{\boldsymbol{R}}^*\left(\overline{y_1} + \overline{\Delta}, \boldsymbol{d}\right)\right] = 0 \quad [8.11]$$

$$[\boldsymbol{e} - \boldsymbol{R}(y_1 + \Delta, \boldsymbol{d})] \cdot [\boldsymbol{e}^* - \boldsymbol{R}^*(y_1 + \Delta, \boldsymbol{d})] = 0 \quad [8.12]$$

$$\frac{1}{\mu}\boldsymbol{n}(\boldsymbol{e}, \boldsymbol{d}) \cdot \boldsymbol{e}^* + S^*(\boldsymbol{e}, \boldsymbol{d}) = 0 \quad [8.13]$$

The design sensitivities $\boldsymbol{e}^*$ can be solved from 8.11, 8.12 and 8.13. By a successive application of the above equations the design sensitivities can be evaluated for the entire fabric.

8.3.5 Examples

A test example often considered is a thermoformed hemisphere. A typical simulation result is shown in Fig. 8.14(a). The initial warp and weft yarns are taken as geodetic lines. The starting point for these yarns is taken as the pole of the sphere. In Fig. 8.14(b) a thermoformed hemisphere is shown.

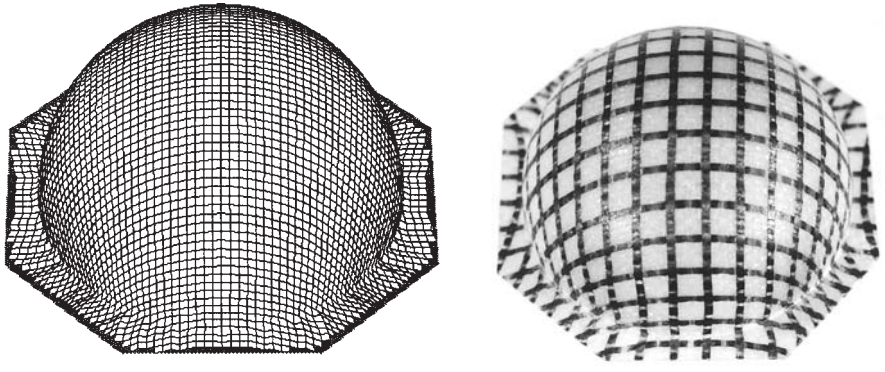

8.14 Draping simulation for a hemispherical surface: (a) grid representing the local yarn orientations; (b) experimental result using a hybrid reinforcement.

As a simple example used to test the evaluation of design sensitivities, draping on an undulated surface is considered. The obvious orientations of the yarns as found by the simulation are depicted in Fig. 8.15(a). The design variable being considered is the blank orientation. In Fig. 8.15(b) the design sensitivities for this design variable are shown. It is stressed that these design sensitivities are obtained by direct application of 8.11, 8.12 and 8.13, rather than using finite differences.

8.4 Finite element simulation

8.4.1 Introduction

For many practical applications it is necessary to satisfy certain mechanical behaviour constraints. Stress and strain criteria may be applied to guarantee that no failure occurs during normal operating conditions. Other constraints may reflect tolerable deflections and stability of the structure. Similar to the production process, numerical simulations may be used to investigate the mechanical behaviour of a CFRTP component or structure. Generally, such numerical simulations are carried out using finite element models. In many cases the CFRTP products at hand can be identified as being thin walled. Therefore, finite shell elements are the best candidates to use in the corresponding finite element models.

Before a finite element analysis can be carried out, information on the material must be provided. For CFRTP products the laminate stiffnesses are determined by the local fibre orientations. As discussed in Section 8.3, these fibre orientations differ generally from place to place. Therefore, these orientations must be determined prior to a finite element analysis. Subsequently, the laminate stiffnesses must be evaluated using the properties of the constituents and the local fibre orientations. As little information on the evaluation of laminate stiffnesses for sheared CFRTP material can be found in the literature, we shall address this aspect in Section 8.4.2.

In Section 8.4.3 some details on modelling thin-walled structures and in particular CFRTP products will be given. Since finite element analysis of thin-walled structures is described in many textbooks, little attention will be paid to this aspect. To a lesser extent the same holds true for design sensitivity analysis using finite element models.

8.4.2 Laminate stiffnesses for thermoformed CFRTP composites

The correct determination of the mechanical material properties is a complicated problem. Often, the way to obtain strength and stiffness data is by

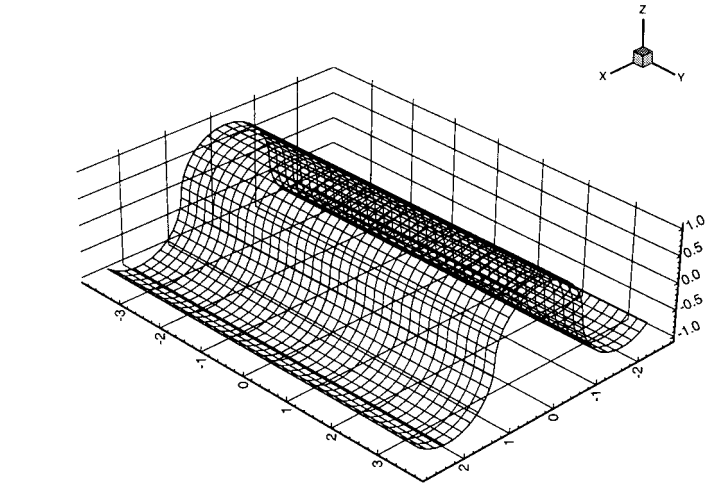

a)

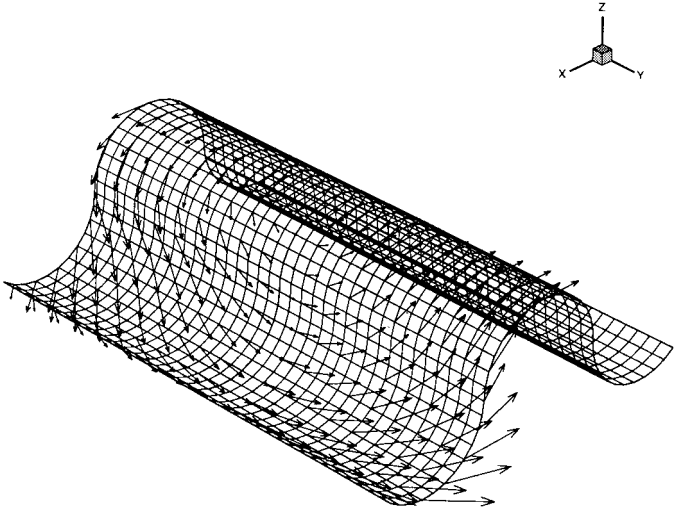

b)

8.15 (a) Draping simulation for an undulated surface. (b) Design sensitivities corresponding to the initial blank orientation.

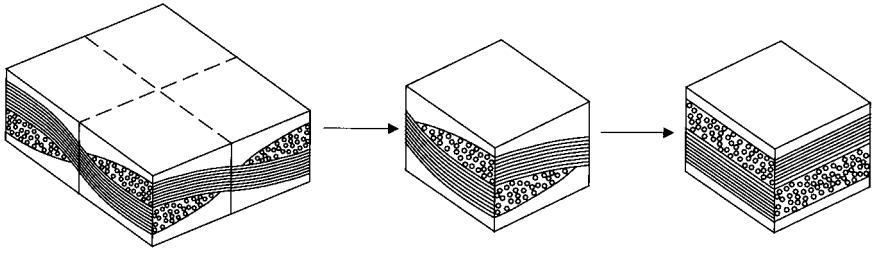

8.16 Transformation of a repeating cell into a four-layered laminate.

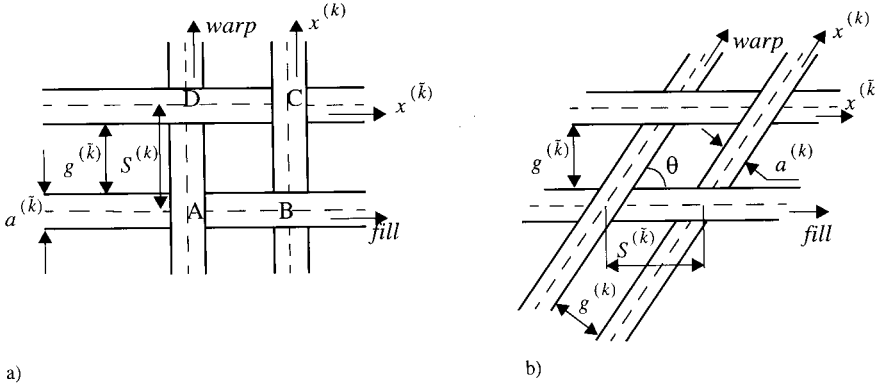

8.17 Assumed strand configuration in the undeformed (a) and deformed (b) states.

experiment [4]. This is because of the complex structure of CFRTP and the large influence of the manufacturing process on the local mechanical properties. The large number of parameters controlling the material properties makes it too expensive and impractical to characterize CFRTP through experiments only. Therefore, the necessity of theoretical models, which can predict the material properties of CFRTP accurately, becomes evident.

The simplest woven fabric (WF) pattern is the plain weave (Figs. 8.16 and 8.17). A number of parameters determine the WF laminate structure, e.g. the fibre undulation, presence of a gap between adjacent strands, actual cross-sectional geometry of the strands and the strand fibre volume fractions.

Various mathematical models have been proposed to describe the thermo-elastic properties of plain weave WF composites. Ishikawa and Chou [28] presented so-called mosaic and fibre undulation models, which apply classical laminate theory (CLT) for every infinitesimal piece of a repeating region of a WF lamina. The mosaic model idealizes the WF lamina

as an assemblage of pieces of asymmetrical cross-ply laminates, which are stacked under iso-strain or iso-stress conditions. This model does not consider the strands' undulation. It was noted by Rai [29] and Vu-Khanh and Liu [30] that the fibre undulation effect cannot be neglected. The fibre undulation model by Ishikawa and Chou [28] takes into account the undulation in one direction only. It is assumed that the strand geometry in the perpendicular direction does not vary. This model gives a satisfactory agreement between experiment and numerical prediction for the elastic moduli in the undulation direction, but the elastic properties in the transverse direction are not valid.

Zhang and Harding [31] presented a plain weave fabric model based on the strain energy equivalence principle. A finite element model is used to evaluate the effective elastic properties. Again, the undulation is considered in one direction only. Another drawback is that it involves substantial computations.

Kabelka [32] proposed a 2-D analytical model considering the undulation in both the warp and fill directions. A laminate is modelled as an assemblage of unidirectional (UD) warp and fill strands and a matrix layer. Considering the strand undulation, equivalent UD lamina properties are determined. Global elastic coefficients are defined on the basis of CLT. The actual strand cross-sectional geometry is ignored. The method gives a higher stiffness because the maximum strand thickness is used for calculations.

Naik *et al.* published a series of papers [33–36] on refined plain fabric composite models. These models take into account the undulation of both the warp and fill strands and the actual strand cross-sectional geometry. The obtained results are in agreement with the experimental results.

All above models are restricted to orthogonal weave structures. Therefore, these models are inadequate for thermoformed CFRTP products. In the present section, the analytical model of Polynkine and Van Keulen [37] for predicting the elastic properties of sheared plain weave composites is described. The approach is essentially based on the 2-D geometric representation of a plain single-layer WF composite proposed by Naik and Ganesh [34,35].

The model proposed in [37] requires four subsequent steps. Firstly, the equivalent properties, e.g. mean thicknesses and volume fractions, have to be calculated for each layer. It is emphasized that these properties depend on the actual weave geometry and the shear angle. Secondly, the equivalent elastic properties of the individual layers are computed using the composite cylinder assemblage (CCA) model given by Hashin [38]. Thirdly, the equivalent engineering constants according to the CCA model should be corrected for the effect of crimp, since the CCA model yields the elastic properties of straight strands. Finally, using the equivalent layer properties

and the equivalent engineering constants, the effective elastic laminate stiffnesses can be computed using CLT. To account for multiple layers, it is convenient to subsequently solve the first three steps for each layer and then apply CLT to all sub-layers.

Geometric consideration

Before deriving expressions for the equivalent layer properties, the geometry of the repeating volume element will be described in more detail. The repeating cell is selected as ABCD, as shown in Fig. 8.17(a). For reasons of symmetry, only one quarter of the repeating cell will be considered. This part will be referred to as the unit cell. The unit cell will be transformed into a four-layered laminate as depicted in Fig. 8.16. In this way the coupling between membrane and bending behaviour cannot be described correctly. However, for a multilayered laminate, this coupling can be described, provided that a sufficient number of layers is available and/or the fabric reinforcements are sufficiently thin.

In the initial undeformed configuration (Fig. 8.17a), mutually perpendicular strands (warp and fill) are assumed. In the deformed state, the intersecting angle is changed to $\pi/2 - \theta$ as depicted in Fig. 8.17(b). The angle θ will be referred to as the *shear angle*. Furthermore, it is assumed that the warp and fill strands in the fabric have a quasi-elliptical cross-sectional shape [34], i.e. their shape can be described by sinusoidal functions.

The assumptions adopted for the material model are similar to those introduced for the geometrical simulation algorithms, as discussed in Section 8.3. With these assumptions, the geometry of the strands in the unit cell is characterized by the following parameters, which are also depicted in Figs. 8.17 and 8.18:

$S^{(k)}$ = the strand lengths in the unit cell,
$a^{(k)}$ = the width of the strands,
$g^{(k)}$ = the gap between two adjacent strands $g^{(k)} \geq 0$,
$h^{(k)}$ = the maximum thickness of the strands,
h^{m} = the minimum thickness of the matrix,
H = the total thickness,
$\varphi^{(k)}$ = the local crimp angle,
$\varphi^{(k)}_{\max}$ = the maximum crimp angle,
k = index which relates the above quantities to the warp ($k = 1$) and fill ($k = 2$) strands.
$\tilde{k}$ = index, which refers to the opposite yarn, i.e. $\tilde{k} = 1$ if $k = 2$ and $\tilde{k} = 2$ if $k = 1$.

Now it is possible to derive expressions for the equivalent layer properties. A significant aspect of the shearing of a fabric reinforced laminate is

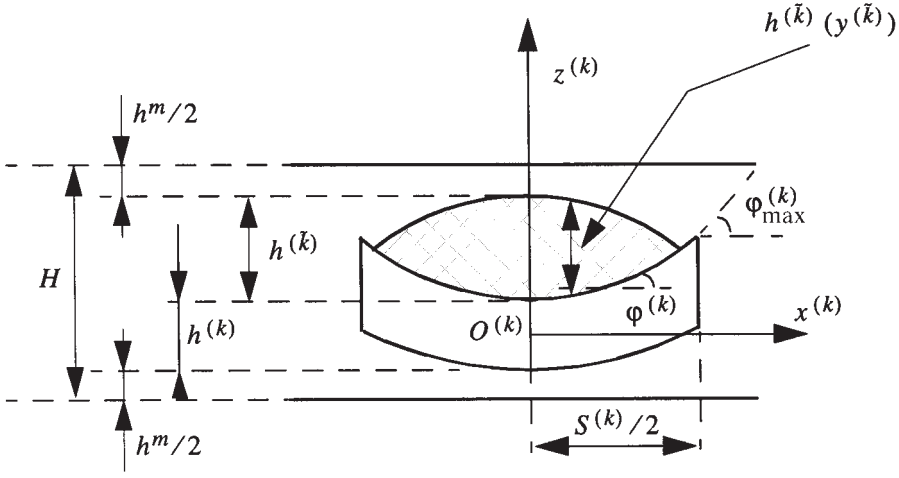

8.18 Cross-section of the unit cell which is taken in the *k*-direction.

the change in thickness. Because of the constant material volume assumption, the thickness must increase during shearing deformation [4]. The actual thickness then becomes:

$$H = \frac{H_0}{\sin(\theta)} \qquad [8.14]$$

where H_0 is the total thickness in the undeformed configuration. Similar expressions can be derived for the mean thicknesses of the yarns as a function of the shear angle. From Fig. 8.17 immediately follows:

$$g^{(k)} = S^{(\tilde{k})} \sin\theta - a^{(k)} \qquad [8.15]$$

If the gap is present, i.e. $g^{(k)} > 0$, the width $a^{(k)}$ and the thickness $h^{(k)}$ of the strands are assumed to be constant:

$$a^{(k)} = a_0{}^{(k)}, \quad \text{and} \quad h^{(k)} = h_0{}^{(k)} \qquad [8.16]$$

Assuming no strand penetration, a quasi-elliptical cross-sectional shape and a constant cross-sectional area, the following relations must hold after gap closure, i.e. $g^{(k)} = 0$:

$$a^{(k)} = S^{(k)} \sin\theta = a_0{}^{(k)} \frac{\sin\theta}{\sin\alpha} \qquad [8.17]$$

$$h^{(k)} = h_0{}^{(k)} \frac{\sin\alpha}{\sin\theta}, \quad \text{with} \quad \sin\alpha = a_0{}^{(k)} \Big/ S^{(\tilde{k})} \qquad [8.18]$$

Here α is the shear angle where the gap becomes zero. Equations 8.17 and 8.18 describe the strand width and thickness as a function of the shear angle θ.

To derive an expression for the mean value of the strand thickness, it is necessary to know the shape of the strand cross-section. Experimental observations [4,29,33,34] have shown that sinusoidal functions yield good approximations of the actual geometry of plain weave fabric lamina cross-sections. Therefore, the following shape functions for the yarn cross-section are used (see Fig. 8.18):

$$h^{(k)}(y^{(k)}) = h^{(k)} \cos\left(\frac{\pi y^{(k)}}{a^{(k)}}\right) \qquad [8.19]$$

Here, the mean thickness can be expressed as

$$\bar{h}^{(k)} = \frac{2h^{(k)}a^{(k)}}{\pi[a^{(k)} + g^{(k)}]} \qquad [8.20]$$

Using 8.15–8.18, it can be shown that

$$\bar{h}^{(k)} = \frac{\bar{h}_0^{(k)}}{\sin\theta}, \quad \text{where } \bar{h}_0^{(k)} = \frac{2}{\pi} h_0^{(k)} \sin\alpha \qquad [8.21]$$

After evaluating the effective thicknesses of the warp and fill strands according to 8.20, the thickness of the pure matrix layer is estimated by the remaining thickness, i.e.

$$\bar{h}^{\mathrm{m}} = H - \left(\bar{h}^{(k)} + \bar{h}^{(\tilde{k})}\right) \qquad [8.22]$$

where H is the total thickness of the fabric unit cell.

Calculation of effective elastic laminate stiffnesses

The calculating procedure is performed by substituting the woven fabric reinforced composite by an equivalent four-layered laminate, i.e. an asymmetric angle-ply lamina between two pure matrix layers. In this method, the mean thicknesses of the strands obtained from equations 8.20–8.22 are taken as the thicknesses of the respective laminae.

The equivalent properties of the individual layers

$$E_{\mathrm{L}}^{(k)}, E_{\mathrm{T}}^{(k)}, \nu_{\mathrm{LT}}^{(k)}, G_{\mathrm{LT}}^{(k)}, G_{\mathrm{TT}}^{(k)} \qquad [8.23]$$

are evaluated by using the CCA model given by Hashin [38]. This model is probably the most commonly used for definition of the effective properties of fibre reinforced materials. Applying the CCA model [34,38], the values (8.23) are determined from the transversely isotropic fibre (subscript f)

properties $E_{fL}^{(k)}$, $E_{fT}^{(k)}$, $\nu_{fLT}^{(k)}$, $G_{fLT}^{(k)}$, $G_{fTT}^{(k)}$ and the isotropic matrix (subscript m) properties E_m, ν_m, and the corresponding strand fibre volume fractions. Subscripts L and T denote unidirectional composite elastic properties along the fibre and transverse fibre directions.

The experimentally determined fibre volume fraction of a CFRTP laminate is the overall fibre volume fraction v_f^0, i.e. the ratio of the volume of fibres with respect to the total volume of the laminate. In the present analysis, the strands are idealized as equivalent UD laminae. Therefore, the fibre volume fractions in such UD laminae with effective elastic properties (8.23) are referred to as the strand fibre volume fractions v_f^s. The latter is the ratio of the fibre volume with respect to the strand volume. Knowing the overall fibre volume fraction v_f^0 of a laminate and the strand volumes, the strand fibre volume fraction v_f^s can be obtained.

The CCA model yields the elastic properties of straight strands with a specified strand fibre volume fraction. Thus, the undulation of the warp and fill strands will be brought into account using the technique described by Lekhnitskii [39], which is based on a transformation of the compliances. After this transformation, the locally reduced compliances $S'_{ij}(\varphi)$ are averaged over the length of the strands to determine the effective compliances of the strands. As an approximation, the mean value of the compliance can be defined in the interval $(0, \varphi_{max})$ [32,34]:

$$\overline{S}_{ij} = \frac{1}{\varphi_{max}} \cdot \int_0^{\varphi_{max}} S'_{ij}(\varphi) d\varphi, \quad i, j = 1, 2, 6 \qquad [8.24]$$

The integration 8.24 is made under the assumption that in an actual lamina φ_{max} is very small, and the functions $\sin\varphi$ and $\cos\varphi$ can be replaced by the first terms of their Taylor series. Finally, the effective elastic constants of the strands are given by [37]:

$$\overline{E}_L^{(k)} = \frac{E_L^{(k)}}{1 + \frac{\varphi^2{}_{max}^{(k)}}{3}\left[\frac{E_L^{(k)}}{G_{LT}^{(k)}} - \left(2\nu_{LT}^{(k)}\right)\right]}, \quad \overline{E}_T^{(k)} = E_T^{(k)}$$

$$\overline{\nu}_{TL}^{(k)} = \nu_{TL}^{(k)} + \frac{\varphi^2{}_{max}^{(k)}}{3}\left(\nu_{TT}^{(k)} - \nu_{TL}^{(k)}\right)$$

$$\overline{G}_{LT}^{(k)} = \frac{G_{LT}^{(k)}}{1 + \frac{\varphi^2{}_{max}^{(k)}}{3}\left[\frac{G_{LT}^{(k)}}{G_{TT}^{(k)}} - 1\right]} \qquad [8.25]$$

Notice that the straight fibre moduli are retrieved from 8.25 when $\varphi_{max} \to 0$.

Now the stress–strain relations as used in the CLT become:

$$\begin{bmatrix} \sigma_x \\ \sigma_y \\ \sigma_{xy} \end{bmatrix}^{(k)} = [Q]^{(k)} \begin{bmatrix} \varepsilon_x \\ \varepsilon_y \\ \gamma_{xy} \end{bmatrix}^{(k)},$$

$$\text{with } [Q]^{(k)} = \begin{bmatrix} \dfrac{\overline{E}_{\mathrm{L}}{}^{(k)}}{D^{(k)}} & \dfrac{\overline{\nu}_{\mathrm{LT}}{}^{(k)}\overline{E}_{\mathrm{L}}{}^{(k)}}{D^{(k)}} & 0 \\ \dfrac{\overline{\nu}_{\mathrm{LT}}{}^{(k)}\overline{E}_{\mathrm{L}}{}^{(k)}}{D^{(k)}} & \dfrac{\overline{E}_{\mathrm{T}}{}^{(k)}}{D^{(k)}} & 0 \\ 0 & 0 & \overline{G}_{\mathrm{LT}}{}^{(k)} \end{bmatrix} \quad [8.26]$$

with $D^{(k)} = 1 - \overline{\nu}_{\mathrm{LT}}{}^{(k)}\overline{\nu}_{\mathrm{TL}}{}^{(k)}$, $k = 1, 2$. The effective moduli for an isotropic material under plane stress conditions are taken for the matrix material.

Knowing the thicknesses of all layers and the reduced effective moduli, the contribution to the equivalent laminate stiffnesses can be calculated using CLT and appropriate transformations to account for the orientations of the equivalent reinforcement layers. Note that at this stage the whole unit cell is modelled as an asymmetrical angle-ply laminate. Consequently, for a single reinforcement layer the coupling matrix will be set to zero. In case of multiple reinforcement layers, the present approach will be repeated for each layer.

8.4.3 Finite element analysis

The thermoplastic products being considered in the present chapter are thin walled. Provided that the smallest local wavelength of the deformation pattern is sufficiently large compared with the wall thickness and moreover the smallest principal radius of curvature is large compared with the wall thickness, thin shell theory can be used as a starting point for mechanical analyses. In standard textbooks, several finite elements for thin shells can be found, see [40–42] among others. Examples presented in the present chapter were all obtained with the triangular shell element as described in [43] and the references given therein. When the smallest wavelength becomes too small it may be necessary to account for transverse shear deformations. The simplest theory accounting for transverse shear deformations is the Mindlin–Reissner theory. Many other higher-order theories with increasing complexity have been reported in literature, see for example [44].

Finite element analysis of CFRTP products is, as mentioned earlier, somewhat hindered by the fact that laminate stiffnesses must be specified that differ from place to place. As discussed in Section 8.3, the simulation of the forming process can be based on a geometrical algorithm, for which gen-

erally a rectangular grid of crossover points is used. The requirements for this grid are entirely different from those for the finite element mesh as compared. The most striking differences are the following:

- The grid size for the geometrical forming simulation is mainly determined by local details to be included in the forming simulation. For the finite element mesh, the required mesh density is in addition determined by the local stress and strain gradients.
- Generally, when a geometrical forming simulation is applied there is no need for a more advanced selection of the local grid size, as the related numerical effort is relatively small. This is in contrast to finite element analysis, for which a graded mesh density is often required to achieve a requested accuracy against acceptable costs.
- The domain being modelled for the forming process is often different from the corresponding finite element model. The latter covers only a sub-domain of the former. The reason for this is that after the forming process, the superfluous material will be removed and the topology may be adapted.

The above differences imply that the fibre orientations cannot be transferred one-to-one from the grid that is being used for the forming simulation to the finite element model. One method is to search for each integration point in the finite element mesh, the closest crossover point available from the grid being applied in the forming simulation. As for the latter, sometimes relatively large grid dimensions can be applied, for which erroneous results may be found. Therefore, using additional checks is recommended. An efficient approach is to check the angle between the normal vectors to the surface at the crossover point and the integration point. If this angle differs too much from zero, then the crossover point found is to be rejected.

In the context of structural optimization, the finite element model can be used to evaluate design sensitivities [27]. The simplest approach towards design sensitivities is by means of global finite difference techniques. The major disadvantage is that for each design variable an additional finite element solution must be determined. This makes the method inefficient. Analytical design sensitivities are accurate and efficient. Their implementation is, however, involved. A compromise between the above methods is the so-called semi-analytical method [27]. In the linear regime the starting point is the well-known equation

$$K(d)\boldsymbol{u}(d) = \boldsymbol{f}(d) \qquad [8.27]$$

where K is the system matrix, $\boldsymbol{u}$ is the vector of nodal degrees of freedom and $\boldsymbol{f}$ is the vector of nodal loads. For simplicity we have assumed a single design variable, which is denoted d. Differentiation of 8.27 gives

$$\frac{\partial \boldsymbol{u}}{\partial d} = K^{-1}\left[\frac{\partial \boldsymbol{f}}{\partial d} - \frac{\partial K}{\partial d}\boldsymbol{u}\right] \quad [8.28]$$

The term $\partial \boldsymbol{f}/\partial d - (\partial K/\partial d)\boldsymbol{u}$ is often referred to as the pseudo-load vector. This pseudo-load vector is generally evaluated at element level, using central or forward finite differences for $\partial K/\partial d$. The implementation of the semi-analytical method is relatively easy and the efficiency is good. A severe disadvantage is its sensitivity with respect to large rigid body motions for individual elements. Adequate remedies, which do not spoil its efficiency, have been proposed [45,46]. Once $\partial \boldsymbol{u}/\partial d$ has been obtained, the design sensitivities for strains and stresses can be evaluated straightforwardly.

Application of the semi-analytical method to CFRTP products requires additional information on the design sensitivities of the fibre orientations, as discussed in Section 8.3. Subsequently, corresponding design sensitivities for the laminate stiffnesses can be determined straightforwardly.

8.5 Optimization of CFRTP products

8.5.1 Introduction

As indicated in the previous sections, the design of thermoplastic products with a continuous fibre reinforcement is a difficult task. The designer not only has to meet the (mechanical) behaviour constraints, such as stability and upper limits on stresses and strains, but in addition restrictions are imposed by the applied forming process. This makes the effects due to changes of shape and topology and changes in the processing parameters difficult to predict intuitively. Consequently, controlling a design process towards an optimal solution manually becomes a difficult or even impossible task. Therefore, application of automated optimization techniques is required.

In general, an optimization problem can be formulated as

$$\min[F_0(\boldsymbol{x})] \quad [8.29]$$

subject to

$$F_j(\boldsymbol{x}) \leq 1, \quad (j = 1, \ldots, M), \quad A_i \leq x_i \leq B_i, \quad (i = 1, \ldots, N) \quad [8.30]$$

Here $\boldsymbol{x}$ is a vector of design variables; $F_0(\boldsymbol{x})$ is the objective function; $F_j(\boldsymbol{x})$, $(j = 1, \ldots, M)$ are the normalized constraint functions; A_i and B_i are the lower and upper limits on the design variables, respectively. The objective function typically reflects the costs of a structure or weight. The constraint functions could reflect limits on deflections, strains, stresses, etc. In the present setting they also reflect the manufacturability. When

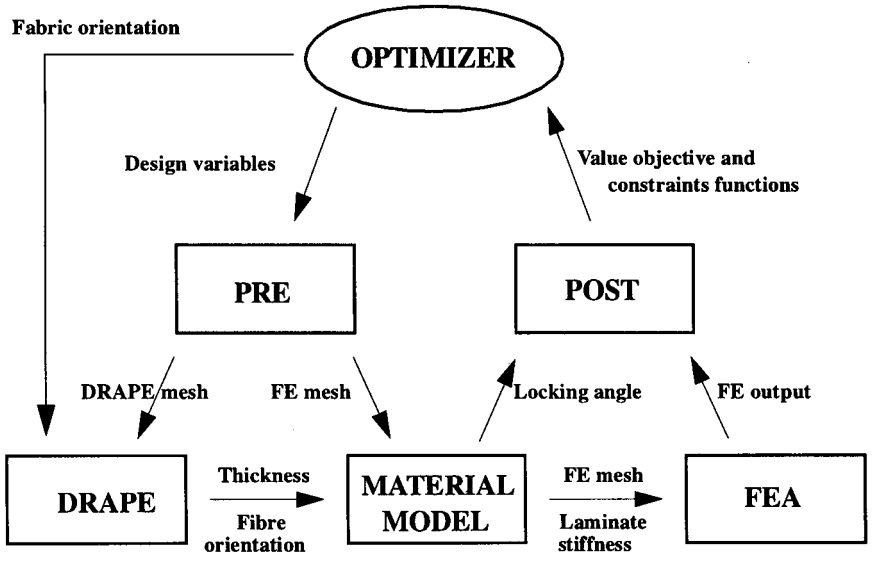

8.19 Combination of optimization, pre- and post-processing, simulation of forming process and finite element analysis for continuous fibre reinforced thermoplastic products.

geometrical forming simulations are applied, the latter constraint is determined by the ratio between the absolute value of the shearing angle and the locking angle. The design variables could reflect parameters controlling the shape of the product, but also the initial position and orientation of the blank.

Application of an automated optimization technique to 8.29 and 8.30 leads, for CFRTP materials, to a combination of the simulation and optimization tools as shown in Fig. 8.19. From this scheme it is seen that the mesh generator, which operates on a parametric model description, is used for both the triangulations of the die and the actual finite element model. The optimizer interacts with the simulation tools directly and through the mesh generator.

Owing to the fact that a sequence of simulation is applied, accumulation of errors can occur. This causes the response function to become noisy. This will be illustrated on the basis of a simple optimization example, which is formulated as maximization of the strain energy of the conical shell with a constant volume requirement. Design variables are the height of the cone (x_1) and the base radius (x_2). At the top of the cone the radius must be kept unchanged and specified by a value of 10 mm. The top surface of the structure is loaded by a pressure load of $p = 0.1\,\mathrm{N/mm^2}$. Owing to symmetry only

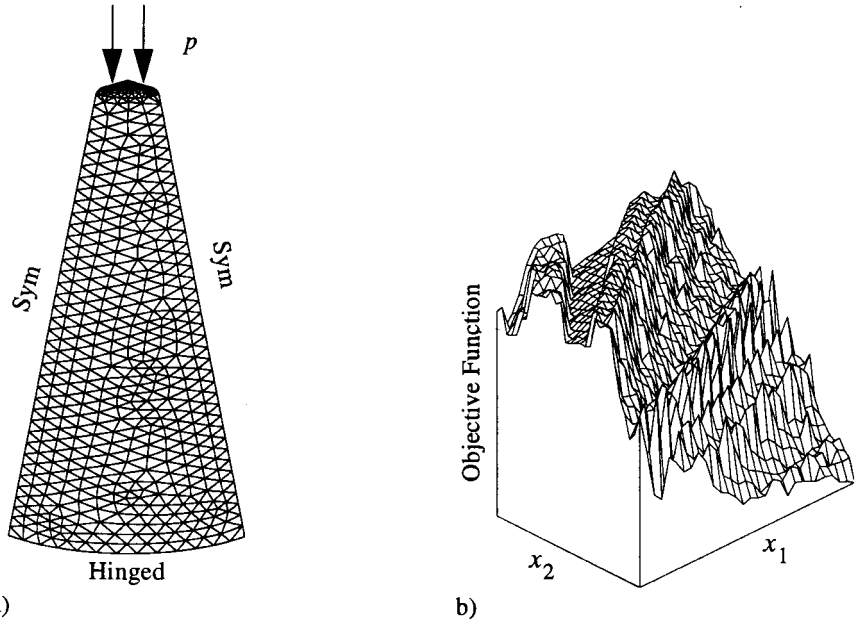

8.20 (a) Conical shell made from CFRTP material. (b) Objective function for the CFRTP conical shell problem.

one quarter of the structure is analysed. A typical configuration and corresponding finite element mesh are depicted in Fig. 8.20(a). The behaviour of the response functions was analysed by a series of response evaluations using 30 increments of both design variables. The results for the objective function are shown in Fig. 8.20(b). The present objective function clearly shows a noisy behaviour which, obviously, can have a significant influence on the convergence characteristics of the optimization process.

The above complication indicates that an optimization algorithm has to be applied which is relatively insensitive with respect to noisy response evaluations. In Section 8.5.2 the so-called multipoint approximation method will be outlined, which satisfies this requirement.

8.5.2 Multipoint approximation method

The basic idea behind the multipoint approximation method [47–50] is to replace the initial optimization problem 8.29–8.30 by a sequence of approximate optimization problems. For the latter, the implicit response functions F_j are replaced by approximate explicit functions $\overline{F}_j(\boldsymbol{x})$. Typically linear and multiplicative approximation functions will be used, but virtually any struc-

ture of approximate functions is possible. The initial optimization problem 8.29–8.30 is now replaced by:

$$\min\left[\overline{F}_0^{(k)}(\boldsymbol{x})\right] \qquad [8.31]$$

subject to

$$\overline{F}_j^{(k)}(\boldsymbol{x}) \leq 1, \quad (j = 1, \ldots, M), \quad A_i^{(k)} \leq x_i \leq B_i^{(k)}$$
$$A_i \leq A_i^{(k)}, \quad B_i^{(k)} \leq B_i, \quad (i = 1, \ldots, N) \qquad [8.32]$$

where k is the current iteration number. The current move limits $A_i^{(k)}$ and $B_i^{(k)}$ define a search sub-region of the design variable space. The $(k + 1)$th iteration is started from $\boldsymbol{x}^{(k)}$ which is the solution of 8.31 and 8.32. The size and location of the next search sub-region depend on the quality of the approximations, the location of the point $\boldsymbol{x}^{(k)}$ in the current search sub-region and the optimization history. A detailed description of the move limit strategy can be found in [51–53].

The approximation functions $\overline{F}_j^{(k)}(\boldsymbol{x})$ are determined using a weighted least-squares method [54], for which only function evaluations can be taken into account and information on the design sensitivities [47–50]. The selection of the weight factor must be done carefully. Details on the selection of the weight factors are given in [51–53].

Because of the fact that a weighted least-squares method is applied, the multipoint approximation method becomes relatively insensitive to noisy response functions. A further advantage of the method is that it can still be used when no information on design sensitivities is available.

8.5.3 Implementation

The starting point for design optimization of a continuous fibre reinforced product is a parametric description of both the actual product and the die surface. The former is generally a subset of the latter. These parametric descriptions typically consist of a collection of interconnected primitives. The parametric descriptions together with a set of design parameters will be used to generate a non-parametric description, this being the input for the preprocessor. The preprocessor is then invoked to generate (a) a representation of the die surface and (b) an appropriate finite element mesh. As mentioned before, the requirements for these meshes may be totally different.

After a representation of the die is generated, a simulation of the draping process is carried out. The local fibre orientations are used to evaluate the local laminate stiffnesses. Once laminate stiffnesses are calculated, the finite element simulation can take place. As shown in Fig. 8.19, objective and constraints functions are determined by the material model and the finite

element model. With a post-processor, the relevant information is retrieved from the finite element solution and passed on to the optimizer.

When design sensitivity information is available, the scheme in Fig. 8.19 becomes slightly more complicated. In that case, design sensitivities are passed from the forming simulation to the material model and subsequently to the finite element analysis. Afterwards, the design sensitivities are used by the optimizer.

8.5.4 Example

A panel with a hole and flanged edges is redesigned with respect to its shape. Figure 8.21 shows a symmetric quarter segment of the panel analysed, the corresponding boundary and loading conditions, and the finite element mesh. As depicted, the upper plate is connected with the flanges by means of a cylindrical surface, and the edge of the hole is reinforced by a part of a torus.

The objective is to minimize the volume of the structure under displacement, strain and linear buckling constraints. Design variables represent the radius of the hole x_1, the width of the upper plate x_2 and the flange width x_3, respectively. The structure is assumed to be thermoformed of E-glass/epoxy composite material. The warp and fill strands of the fabric were prescribed to be parallel to the X and Y co-ordinate directions, respectively, as depicted in Fig. 8.22(b). More details on the precise formulation of the optimization problem can be found in [55].

For the optimal solution, which was obtained after five iterations, the volume of the structure is reduced from 766.2 mm^3 to 486.5 mm^3.

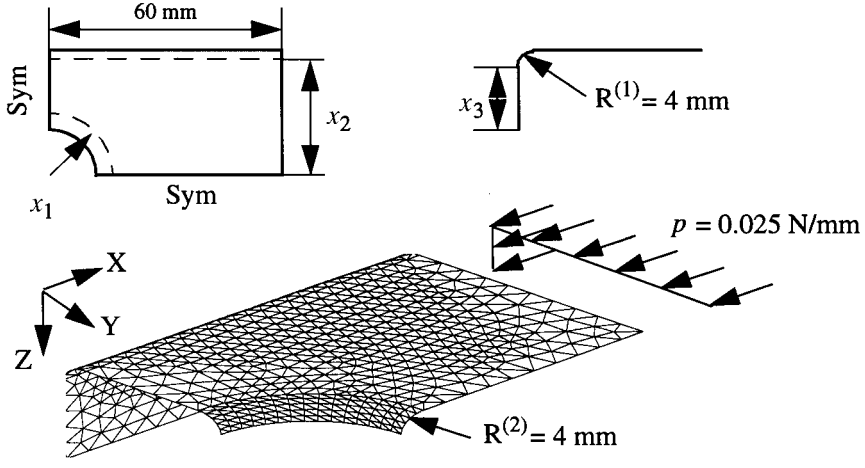

8.21 A panel with a hole and flanged edges.

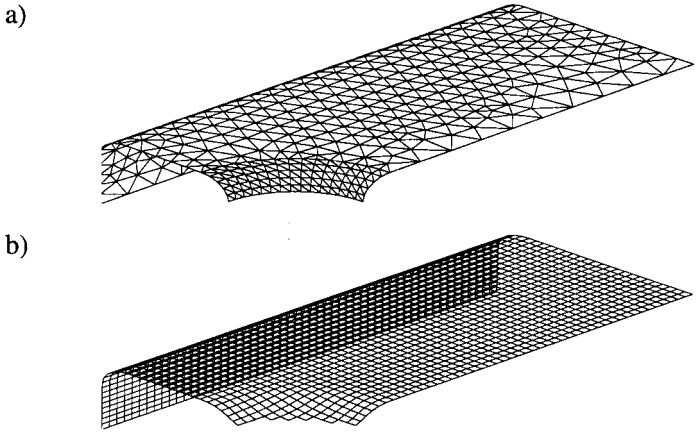

8.22 The optimal configuration of the panel with a hole and flanged edges: (a) the finite element mesh; (b) the orientation of the yarns.

8.6 Conclusions

Composites combine the attractive properties of different materials, e.g. high mechanical and physical performance of fibres and the appearance, bonding and physical properties of polymers. Through this marriage, the poor capacities and drawbacks of the individual components often disappear, like the poor mechanical properties of polymers in general and fibres in compression. To justify the higher cost of this class of materials compared with other engineering materials, such as metals, the price-performance of a design must be competitive. Developments with respect to (minimum energy) structure design and manufacturing of composite components are therefore important. Tools for analysis, design and optimization which are under development must be user-friendly (labour cost), fast (time to market) and able to show designers and analysts in an easy way the effects of variations of the design variables on process parameters, shape, mass, stiffness, strength, durability, etc., to cost.

In this chapter, on the 3-D forming of continuous fibre reinforcements for composites, an outline has been given of the ongoing research at Delft University of Technology. This research is mainly focused on the application of composites in advanced structures. That means the application of high-strength and high-modulus fibres, continuous in length, impregnated up to high volume percentages and with complete control of fibre orientations. The manufacturing processes based on the use of fabrics, such as RTM and press and diaphragm forming, are studied and optimized in such a way that the process control and the desired fibre architecture become part of the entire design process. The straightforward geometrical drape simulation

is a fast and powerful (interactive) tool for the conceptual design phase of composite shell structures, varying from viability and approximate analysis to tool design. In addition, it can be used as a preprocessor to determine the permeability distribution for parts manufactured by resin transfer or resin injection moulding. The program can also be used as a post-processor in several existing CAD systems, and as a drapeability checker and material modeller for the determination of the local engineering constants of the part to be designed. For the embodiment phase of the design process, numerical finite element and design sensitivity calculations are under development as presented. Interactive manipulation, high speed and proper failure criteria are still missing links and therefore important subjects for further developments. Once the interface problems with the process simulation programs are solved and the specific behaviour of rubber dies is formulated in effective algorithms, the design loop can be completed. When this is fast and interactive, realistic integral and concurrent engineering of future advanced composite structure designs becomes possible.

8.7 References

1. McNeill, W.H., 'Human migration in historical perspective', *Population Development Rev*. **10**, 1–18, 1984.
2. Keegan, J., *A History of Warfare*, Pimlico, London, 1993, pp. 126–136, 162–163.
3. Beukers, A., 'Polymer composites versus metals, the structure efficiencies compared', in *SAMPE Proceedings*, Tokyo, 1991, pp. 1113–1120.
4. Robroek, L.M.J., *The Development of Rubber Forming as a Rapid Thermoforming Technique for Continuous Fibre Reinforced Thermoplastic Composites*, Delft University Press, Delft, 1994.
5. Robroek, L.M.J., 'Material response of advanced thermoplastic composites to the thermoforming manufacturing process', paper presented at Proceedings of the Third International Conference on Automated Composites, 15–17 October, 1991, The Hague, the Netherlands.
6. Mack, C. and Taylor, H.M., 'The fitting of woven cloth to surfaces', *J. Textile Inst.*, **47**, T477, 1956.
7. Robertson, R.E., Hsiue, E.S. and Yeh, G.S.Y., 'Fibre rearrangements during the moulding of continuous fibre composites II', *Polymer Composites*, **5**, 191, 1984.
8. Heisley, F.L. and Haller, K.D., 'Fitting woven fabric to surfaces in three dimensions', *J. Textile Inst.*, **2**, 250–263, 1988.
9. Potter, K.D., 'The influence of accurate stretch data for reinforcements on the production of complex structural mouldings', *Composites*, **July**, 1979.
10. Van West, B.P., 'A simulation of the draping and a model of the consolidation of commingled fabrics', PhD Thesis, University of Delaware, 1990.
11. Tam, A.S. and Gutowski, T.G., 'Ply-slip during the forming of thermoplastic composite parts'. *J. Composite Mater.*, **23**, 587–605, 1989.
12. Cogswell, F.N., 'The processing science of thermoplastic structural composites', *Int. Polymer Processing*, **1**(4), 157–165, 1987.
13. Wulfhorst, B. and Horsting, K., *Rechnergestutzte Simulation der Drapierbarkeit*

von Geweben aus HL-Fasern für Faserverbundwerkstoffe (in German), Institut für Textiltechnik der RWTH Aachen, 1991.
14. Bergsma, O.K. and Huisman, J., 'Deep drawing of fabric reinforced thermoplastics', in *Computer Aided Design in Composite Material Technology; Proceedings of the International Conference*, Southampton, Brebbia, C.A., de Wilde, W.P. and Blain, W.R., eds, Springer-Verlag, Berlin, 1988, pp. 323–334.
15. Van West, B.P., Keefe, M. and Pipes, R.B., 'A simulation of the draping of bidirectional fabric over three-dimensional surfaces', *J. Textile Institute*, **81**, 448–460, 1990.
16. Gutowski, T., Hoult, D., Dillon, G. and Gonzalez-Zugasti, J., 'Differential geometry and the forming of aligned fibre composites', *Composites Manufacturing*, **2**(3/4), 147–152, 1991.
17. Van der Weeën, F., 'Algorithms for draping fabrics on doubly-curved surfaces', *Int. J. Num. Meth. Eng.*, **31**, 1415–1426, 1991.
18. Trochu, F., Hammami, A. and Benoit, Y., 'Prediction of fibre orientation and net shape definition of complex composite parts', *Composites: Part A*, **27A**, 319–328, 1996.
19. Aono, M., Breen, D.E. and Wozny, M.J., 'A computer-aided broadcloth composite layout design system', in *Geometric Modeling for Product Realization*, Selected and Expanded Papers from the IFIP TC5/WG5.2 Working Conference on Geometric Modeling, Rensselaerville, NY, USA, 27 September–1 October 1992, Wilson, P.R., Wozny, M.J. and Pratt, M.J., eds, North-Holland, 1992, pp. 223–250.
20. Aono, M., Denti, P., Breen, D.E. and Wozyn, M.J., 'Fitting a woven cloth model to a curved surface: dart insertion', *IEEE Computer Graphics Appl.*, **16**, 60–69, 1996.
21. Bergsma, O.K., 'Three dimensional simulation of fabric draping', PhD Thesis, Faculty of Aerospace Engineering, Delft University of Technology, November 1995.
22. Terzopoulos, D. and Fleischer, K., 'Deformable models', *Visual Computer*, **4**, 306–331, 1988.
23. Collier, J.R., Collier, B.J., O'Toole, G. and Sargand, S.M., 'Drape prediction by means of finite element analysis', *J. Text. Inst.*, **82**(1), 96–107, 1991.
24. Pickett, A.K., Queckbörner, T., De Luca, P. and Haug, E., 'An explicit finite element solution for the forming prediction of continuous fibre-reinforced thermoplastic sheets', *Composites Manufacturing*, **6**, 237–243, 1995.
25. De Luca, P., Lefébre, P. and Pickett, A.K., 'Numerical and experimental investigation of some press forming parameters of two fibre reinforced thermoplastics: APC2-AS4 and PEI-CETEX', paper presented at Fourth Int. Conf. on Flow Processes in Composites Materials FPCM '96, 7–9 September, Aberystwyth, UK, pp. 1–15, 1996.
26. Johnson, A.F. and Pickett, A.K., 'Numerical simulation of the forming process in long fibre reinforced thermoplastics', in *Computer Aided Design in Composite Material Technology V; CADCOMP 96*, Blain, W.R. and De Wilde, W.P., eds, Computational Mechanics Publications, Southampton, pp. 233–242, 1996.
27. Haftka, R.T. and Gürdal, Z., *Elements of Structural Optimization*, 2nd edn, Kluwer, Dordrecht, 1990.
28. Ishikawa, T. and Chou, T.W., 'One-dimensional micro-mechanical analysis of woven fabric composites', *AIAA*, **21**, 1714–1721, 1983.

29. Rai, H.G., Rogers, C.W. and Crane, D.A., 'Mechanics of curved fiber composites', *J. Reinf. Plast. Comp.*, **11**, 552–566, 1992.
30. Vu-Khanh, T. and Liu, B., 'Prediction of fibre rearrangement and thermal expansion behaviour of deformed woven-fabric laminates', *Composites Sci. Technol.*, **53**, 183–191, 1995.
31. Zhang, Y.C. and Harding, J., 'A numerical micromechanics analysis of the mechanical properties of a plain weave composite', *Computer Structures*, **36**, 839–844, 1990.
32. Kabelka, J., 'Prediction of the thermal properties of fibre–resin composites', in *Developments in Reinforced Plastics-3*, Pritchard, G., ed., Elsevier Applied Science, London, 1984, pp. 167–202.
33. Naik, N.K. and Shembekar, P.S., 'Elastic behaviour of woven fabric composites: I–lamina analysis', *J. Composite Mater.*, **26**, 2196–2225, 1992.
34. Naik, N.K. and Ganesh, V.K., 'Prediction of on-axes elastic properties of plain weave fabric composites', *Composites Sci. Technol.*, **45**, 135–152, 1992.
35. Naik, N.K. and Ganesh, V.K., 'Prediction of thermal expansion coefficients of plain weave fabric composites', *Composite Structures*, **26**, 139–154, 1993.
36. Naik, N.K. and Ganesh, V.K., 'An analytical method for plain weave fabric composites', *Composites*, **26**, 281–289, 1995.
37. Polynkine, A.A. and van Keulen, F., *Calculation of Laminate Stiffnesses for Thermoformed Continuous Fibre Reinforced Thermoplastic Composites*, Delft University of Technology, Report LTM 1079, July 1995.
38. Hashin, Z., 'Analysis of composite materials – a survey', *J. Appl. Mech.*, **50**, 481–505, 1983.
39. Lekhnitskii, S.G., *Theory of Elasticity of an Anisotropic Elastic Body*, Holden-Day, San Francisco, 1963.
40. Argyris, J. and Mlejnek, H.P., *Die Methode der Finiten Elementen in der elementaren Strukturmechanik, Band I, Verschiebungsmethode in der Statik*, Friedr. Vieweg, Braunschweig/Wiesbaden, 1986.
41. Bathe, K.J., *Finite Element Procedures in Engineering Analysis*, Prentice-Hall, New Jersey, 1982.
42. Zienkiewicz, O.C. and Taylor, R.L., *The Finite Element Method*, vols 1 and 2, 4th edn, McGraw-Hill.
43. van Keulen, F. and Booij, J., 'Refined consistent formulation of a curved triangular finite rotation shell element', *Int. J. Num. Meth. Eng.*, **39**, 2803–2830, 1996.
44. Noor, A.K. and Burton, W.S., 'Assessment of shear deformation theories for multilayered composite plates', *Appl. Mech. Rev.*, **42**(1), 1, 1989.
45. Olhoff, N., Rasmussen, J. and Lund, E., 'A method of "exact" numerical differentiation for error elimination in finite-element-based semi-analytical shape sensitivity analyses'. *Mech. Struct. Mach.*, **21**, 1–66, 1993.
46. van Keulen, F. and de Boer, H., 'Rigorous improvement of semi-analytical design sensitivities by exact differentiation of rigid body motions', *I. J. Num. Meth. Eng.*, **42**, 71–91, 1998.
47. Toropov, V.V., 'Simulation approach to structural optimization', *Structural Optimization*, **1**, 37–46, 1989.
48. Toropov, V.V., Filatov, A.A. and Polynkine, A.A., 'Multiparameter structural optimization using FEM and multipoint explicit approximations', *Structural Optimization*, **6**, 7–14, 1993.
49. Toropov, V.V., 'Multipoint approximation method in optimization problems with

expensive function values', in *Computational Systems Analysis*, Sydow, A., ed., pp. 207–212, Elsevier, 1992.
50. Toropov, V.V., Filatov, A.A. and Polynkine, A.A., 'Multiparameter structural optimization using FEM and multipoint explicit approximations', *Structural Optimization*, **6**, 7–14, 1993.
51. van Keulen, F., Toropov, V. and Markine, V., 'Recent refinements in the multi-point approximation method in conjunction with adaptive mesh refinement', in *Proceedings of the 1996 ASME Design Engineering Technical Conferences and Computers in Engineering Conference*, 18–22 August, Irvine, CA, McCarthy, J.M., ed., 1996.
52. Toropov, V.V., van Keulen, F., Markine, V. and de Boer, H., 'Refinements in the multi-point approximation method to reduce the effects of noisy structural responses', in *6th AIAA/NASA/ISSMO Symposium on Multidisciplinary Analysis and Optimization*, Bellevue WA, 4–6 September, Part 2, A Collection of Technical Papers, pp. 941–951, 1996.
53. van Keulen, F. and Toropov, V.V., 'New developments in structural optimization using adaptive mesh refinement and multi-point approximations', *Eng. Optimization*, **29**, 217–234, 1997.
54. Draper, N.R. and Smith, H., *Applied Regression Analysis*, 2nd edn, Wiley, New York, 1981.
55. Polynkine, A.A., van Keulen, F., de Boer, H., Bergsma, O.K. and Beukers, A., 'Shape optimization of thermoformed continuous fibre reinforced thermoplastic products', *Structural Optimization*, **11**, 228–234, 1996.